VOLUME 81 SEPARATE No. 606

PROCEEDINGS

AMERICAN SOCIETY
OF
CIVIL ENGINEERS

JANUARY, 1955

DISCUSSION
OF PROCEEDINGS - SEPARATES

281, 296, 300, 330, 333, 375, 387, 396

ENGINEERING MECHANICS
DIVISION

Copyright 1955 by the AMERICAN SOCIETY OF CIVIL ENGINEERS
Printed in the United States of America

Headquarters of the Society
33 W. 39th St.
New York 18, N. Y.

PRICE $0.50 PER COPY

Current discussion of papers sponsored by the Engineering Mechanics Division is presented as follows:

Number		Page
281	The Development of the Turbulent Boundary Layer on Steep Slopes, by William J. Bauer. (September, 1953. Prior discussion: None. Discussion closed)	
	Halbronn, G.	1
	Bauer, William J. (Closure)	7
296	An Experimental Investigation and Limit Analysis of Net Area in Tension, by W. G. Brady and D. C. Drucker. (October, 1953. Prior discussion: None. Discussion closed)	
	Munse, W. H.	11
	Bijlaard, P. P.	12
	Brady, W. G. and Drucker, D. C. (Closure)	16
300	Designing Aluminum Alloy Members for Combined End Load and Bending, by H. N. Hill, E. C. Hartmann, and J. W. Clark. (October, 1953. Prior discussion: 429. Discussion closed)	
	Sawyer, Herbert A., Jr.	23
	Hill, H. N., Hartmann, E. C., and Clark, J. W. (Closure)	27
330	Plastic Deformation of Wide-Flange Beam-Columns, by Robert L. Ketter, Edmund L. Kaminsky, and Lynn S. Beedle. (November, 1953. Prior discussion: 532. Discussion closed)	
	Ketter, Robert L., Kaminsky, Edmund L., and Beedle, Lynn S. (Closure)	31
333	Discussion of Proceedings-Separates 177, 179, 202, 223, 258. (November, 1953)	
	Correction to Discussion of the Application of Heaviside's Step-Function to Beam Problems. Proceedings-Separate 202.	37
375	Deflections of a Circular Beam Out of its Initial Plane, by Enrico Volterra. (December, 1953. Prior discussion: None. Discussion closed)	
	Oesterblom, I.	39
	Volterra, Enrico (Closure)	39
387	An Experimental Study of Bubbles Moving in Liquids, by W. L. Haberman and R. K. Morton. (January, 1954. Prior discussion: None. Discussion closed)	
	Roberson, J. A., Barker, C. L., and Ruff, P. F.	45
396	Discussion of Proceedings-Separates 185, 223, 250, 258, 281. (January, 1954)	
	Correction to Discussion of Applications of the Relaxation Technique in Fluid Mechanics. Proceedings-Separate No. 223.	47
	Correction to Discussion of Mechanics of Manifold Flow. Proceedings-Separate No. 258.	47

Reprints from this publication may be made on condition that the full title of paper, name of author, page reference (or paper number), and date of publication by the Society are given.

The Society is not responsible for any statement made or opinion expressed in its publications.

This paper was published at 1745 S. State Street, Ann Arbor, Mich., by the American Society of Civil Engineers. Editorial and General Offices are at 33 West Thirty-ninth Street, New York 18, N.Y.

Discussion of
"THE DEVELOPMENT OF THE TURBULENT BOUNDARY LAYER ON STEEP SLOPES"

by William J. Bauer
(Proc. Sep. 281)

G. HALBRONN.[14]—A large number of experiments have been performed by Mr. Bauer which were concerned with boundary-layer development on spillways having various conditions of slope and roughness. This phenomenon was previously studied, both theoretically and experimentally.[15] It is of interest to compare the author's results with those obtained from a study of Eq. 3 when u is assumed to follow one of the relationships valid for the velocity distribution in the case of uniform flow within a pipe. The mathematical derivation can be evolved when:

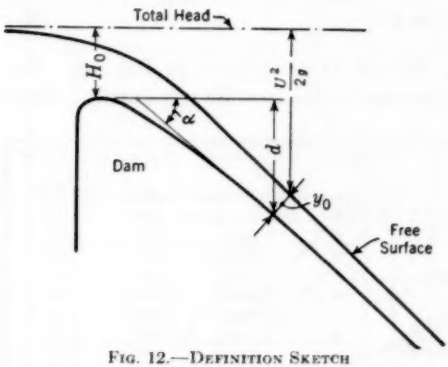

FIG. 12.—DEFINITION SKETCH

(*a*) The region under study is located away from the spillway crest. In this case

$$U = \sqrt{2\,g\,(d + H_0 - y_0 \cos \alpha)} \quad \ldots (23a)$$

can be expressed approximately as

$$U = \sqrt{2\,g\,(d + H_0)} \quad \ldots (23b)$$

The terms in Eqs. 23 are defined in Fig. 12.

(*b*) The spillway, away from the crest, has a constant slope α. It can be seen that the boundary-layer thickness is independent of the flow near the crest and is dependent only on the local conditions. Therefore, the results are general.

When the spillway is smooth, Eq. 4 can be used if

$$\frac{k\sqrt{\frac{\tau_0}{\rho}}}{\nu} < 5 \quad \ldots (24)$$

Letting

$$z = 0.4\,\frac{U}{\sqrt{\frac{\tau_0}{\rho}}} = \frac{0.566}{\sqrt{c_f}} \quad \ldots (25)$$

Eq. 4 can be written as

$$\frac{\delta}{x} = \frac{0.278}{\mathbf{R}_x}\,z\,e^z \quad \ldots (26)$$

in which

$$\mathbf{R}_x = \frac{U\,x}{\nu} \quad \ldots (27)$$

---

[14] Highway and Bridge Engr., 6th Elec. Dept., Grenoble, France.

[15] "Étude de la mise en régime des écoulements sur les ouvrages à forte pente. Application au problème de l'entrainement d'air," by G. Halbronn, *Houille Blanche*, 1952, No. 1, pp. 21–40; No. 3, pp. 347–371; No. 5, pp. 702–722.

Therefore, from Eq. 3,

$$R_x = 4.35\, e^{s}\,(z^2 - 2.8\,z + 4.32) \quad \ldots\ldots (28)$$

The variation of δ/x, as a function of R_x, is given in parametric form by Eqs. 26 and 28. This variation can be approximated by

$$\frac{\delta}{x} = 0.039\, R^{-0.097}{}_x \quad \ldots\ldots (29)$$

for $8.5 < z < 12.5$ $(0.00205 < c_f < 0.00443)$. If it is assumed[16] that

$$\frac{u}{\sqrt{\frac{\tau_0}{\rho}}} = 8.7 \left(\frac{y \sqrt{\frac{\tau_0}{\rho}}}{\nu} \right)^{1/7} \quad \ldots\ldots (30)$$

then

$$\delta = 0.158\, R^{-0.2}{}_x \quad \ldots\ldots (31)$$

The curves corresponding to Eqs. 29 and 31 are shown in Fig. 13. For small values of the Reynolds number, the curves are in close agreement. This

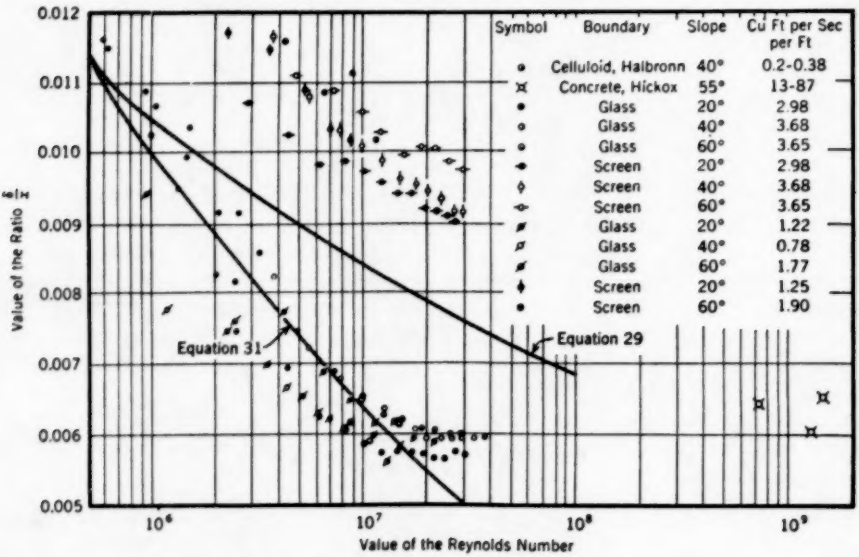

FIG. 13.—THE RATIO $\frac{\delta}{x}$ AS A FUNCTION OF R_x FOR SMOOTH BOUNDARIES

agreement indicates that the application of a logarithmic law to the experiments[15] is proper. In the range of Mr. Bauer's smooth-boundary experiments, Eq. 31 accounts for the observed increase of the thickness of the boundary layer. This agreement is expected as velocity profiles are better approximated

[16] "Modern Developments in Fluid Dynamics," by S. Goldstein, Clarendon Press, Oxford, England, 1952, p. 339.

by an expression such as

$$u = J\, y^{j} \qquad (32)$$

than one in the form:

$$u = b \log_{10} y + c \qquad (33)$$

although, in Fig. 2, j would be equal to 1/7.5. It was also observed that, for large values of the Reynolds number, the velocity profiles do not correspond to the logarithmic law. Because these larger Reynolds numbers occurred downstream from the critical point, it was assumed[15] that the poor agreement was caused by a physical change in the flow. The author's experiments show that this is not true.

It should be noted from Fig. 13 that, when the Reynolds number $\frac{2\,U\,\delta}{\nu}$ exceeds 10^5, the smooth-boundary experimental points depart from Eq. 31 and

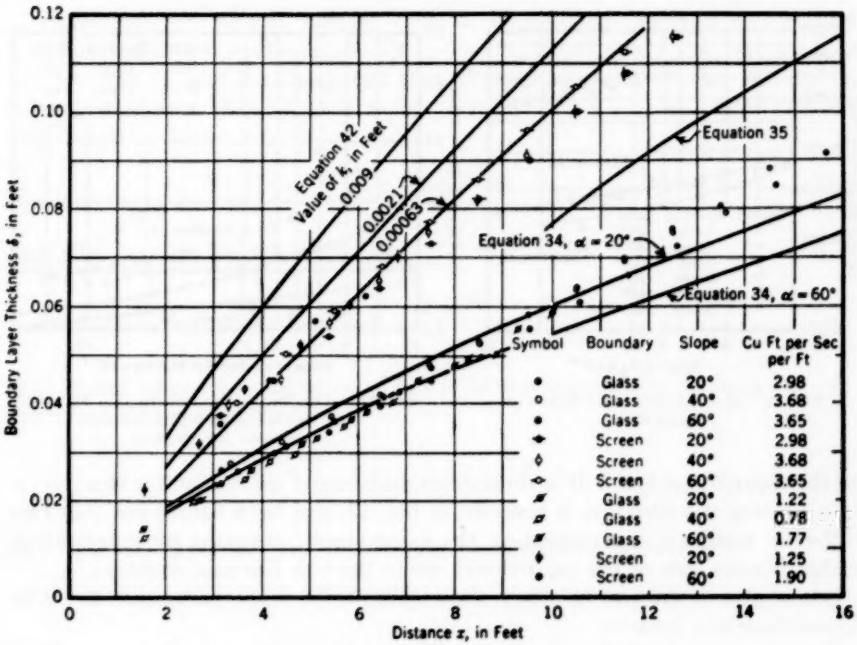

FIG. 14.—THICKNESS OF THE BOUNDARY LAYER AS A FUNCTION OF x

more closely agree with Eq. 29. This value (10^5) is the upper limit for the validity of Blasius' law.

Eq. 31 can also be written as

$$\delta\ (\text{ft}) = \frac{0.0106}{S^{0.1}}\, x\ (\text{ft})^{0.7} \qquad (34)$$

In Fig. 14 the curves corresponding to Eq. 34 for $\alpha = 20°$ and $\alpha = 60°$ are shown. As a result of the exponent 0.1 in Eq. 34, δ is approximately inde-

pendent of S, but this fact has no special physical significance. Curves representing Eq. 29 in the form:

$$\delta \text{ (ft)} = \frac{0.0104}{S^{0.0485}} x \text{ (ft)}^{0.8515} \quad \ldots\ldots\ldots\ldots\ldots\ldots (35)$$

are also shown in Fig. 14. These curves are in superposition.

In Fig. 15 there is shown the relationship between c_f and $\mathbf{R}_\delta$. This relationship is obtained by letting $u = U$ and $y = \delta$ in Eq. 30 to result in

$$c_f = 2\left(\frac{\sqrt{\frac{\tau_0}{\rho}}}{U}\right)^2 = 0.0463\,\mathbf{R}^{-\frac{1}{4}}_\delta \quad \ldots\ldots\ldots\ldots\ldots\ldots (36)$$

The smooth-boundary experimental points in Fig. 15 are farther from the curve of Eq. 36 than the same points are from the curve of Eq. 16 which corresponds

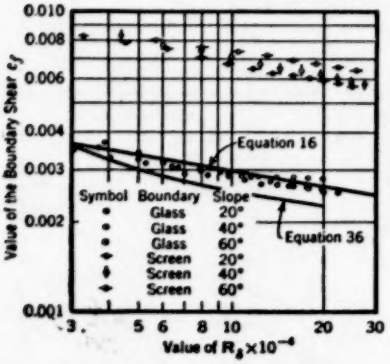

FIG. 15.—THE RELATIONSHIP BETWEEN c_f AND $\mathbf{R}_\delta$

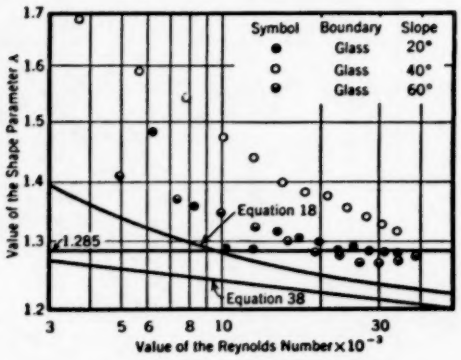

FIG. 16.—THE SHAPE PARAMETER AS A FUNCTION OF THE REYNOLDS NUMBER FOR SMOOTH BOUNDARIES

to the logarithmic law. It is difficult to understand the reason for this deviation because the situation is reversed in Fig. 13, and both figures are only two different methods of representing the same result, obtained by substituting either Blasius' law or the logarithmic law in the von Kármán equation.

It is also of interest to study the values of the shape parameter Λ. The logarithmic law leads to

$$\delta_d = 1.765\sqrt{c_f}\,\delta \quad \ldots\ldots\ldots\ldots\ldots\ldots (37a)$$

and

$$\delta_m = 1.765\sqrt{c_f}\,\delta\,(1 - 3.54\sqrt{c_f}) \quad \ldots\ldots\ldots\ldots\ldots\ldots (37b)$$

Then, from Eq. 16,

$$\frac{\Lambda}{\Lambda - 1} = 1.15\log_{10}\Lambda\mathbf{R} + 0.645 \quad \ldots\ldots\ldots\ldots\ldots\ldots (38)$$

Blasius' law leads to $\delta_d = \frac{\delta}{8}$, $\delta_m = \frac{7}{72}\delta$, and $\Lambda = \frac{9}{7}$. The corresponding curves are plotted in Fig. 16. The experimental points are somewhat scat-

tered; nevertheless, the value $\Lambda = 1.285$ appears to be valid for large values of **R**. The curves for Eqs. 18 and 38 follow the general trend of the experimental points more accurately, although with a systematical displacement. It is worth while to note that the curve for Eq. 38 and the curve for the empirical law (Eq. 18) are in close agreement.

In Fig. 16 the experimental points shown by Mr. Bauer in Fig. 10(*a*) have been plotted exactly as shown in Fig. 10(*a*) with the value of the abscissa changed to "Value of the Reynolds Number $\times 10^{-3}$." Also, in Fig. 16 the curve for Eq. 18 is shown on the basis of the "new" abscissa. This value for the abscissa is correct, rather than Mr. Bauer's "Value of the Reynolds Number $\times 10^{-6}$," as can be seen by introducing into Eq. 18 the value of **R** equal to 10,000 so as to result in Λ equal to 1.287. It is true that introducing a value of **R** equal to 10,000,000 into Eq. 18 results in Λ equal to 1.380, but Messrs. Tetervin and Lin established Eq. 18 only for values of **R** between 1,500 and 40,000.

When $(k/\nu)\sqrt{\tau_0/\rho}$ is greater than 5, dimensional analysis shows that $u/\sqrt{\tau_0/\rho}$ depends simultaneously on $(y/\nu)\sqrt{\tau_0/\rho}$ and y/k. For $(k/\nu)\sqrt{\tau_0/\rho}$ greater than 71, and for the special type of roughness used by Mr. Nikuradse, it has been shown[4] that for uniform flow in a pipe Eq. 5 is valid for the velocity distribution. Therefore,

$$\frac{\delta}{x} = 0.0337\,\frac{k}{x}\,e^{z} \qquad (39)$$

Applying Eq. 3 to Eq. 39 results in

$$e^{z}\left(z - 2.4 + \frac{2.24}{z}\right) = 1.898\,\frac{x}{k} \qquad (40)$$

Eqs. 39 and 40 give the variation of δ/x as a function of x/k (shown in Fig. 17) which can be approximated by

$$\frac{\delta}{x} = 0.0447\left(\frac{x}{k}\right)^{-0.154} \qquad (41)$$

for $6 < z < 9$ $(0.00395 < c_f < 0.0089)$ or, in a dimensional form:

$$\delta = 0.0447\,k^{0.154}\,x^{0.846} \qquad (42)$$

The curves for Eq. 42 are shown in Fig. 14 for $k = 0.009$ ft, $k = 0.0021$ ft, and $k = 0.00053$ ft. This last value of k is seen to be in good agreement with the experimental data. The considerable variation of the values for k given in Fig. 14, in Fig. 9, or by the tests involving uniform flow (although, for a screen made with wire of an 0.0008-ft diameter, an equivalent sand roughness of 0.009 ft seems unexpected) leads one to believe that Eq. 5 does not agree with the observed velocity-profile distribution. In fact, if c_f is determined from the experimental points of Fig. 3 and from Eq. 3 and is then used to plot $u/\sqrt{\tau_0/\rho}$ as a function of y, a single curve does not result, as it would if Eq. 5 were applicable. It would be most interesting to investigate Mr. Bauer's data

on rough bottoms by the method described by Boris A. Bakhmeteff.[17] By plotting $[(u/\sqrt{\tau_0/\rho}) - 5.75 \log_{10} (y/k)]$ as a function of $\log [(k/\nu) \sqrt{\tau_0/\rho}]$, it may be possible to determine the velocity distribution corresponding to the observations. Examination of Figs. 8 and 9 appears to show that $\sqrt{\tau_0/\rho}$ depends on both y/k and $(y/\nu) \sqrt{\tau_0/\rho}$.

Another manner of solving the problem might be by the use of prototype data obtained by the simple method followed by Mr. Hickox.[12] Such results (including a measured value for δ) have been published[18] by V. Michels, A.M. ASCE, and M. Lovely. These results, obtained at the Glennmaggie Dam in Australia, are as follows:

x, in feet	δ, in feet (measured)	δ, in feet (computed)
14	0.147	0.127
39	0.347	0.322
65	0.552	0.525

Plotted in Fig. 17 (with $k = 0.005$ ft for concrete) these points fall between the author's design curve and the curve of Eq. 41. The foregoing listing also shows the values of δ computed by the method used by Mr. Bauer in applying

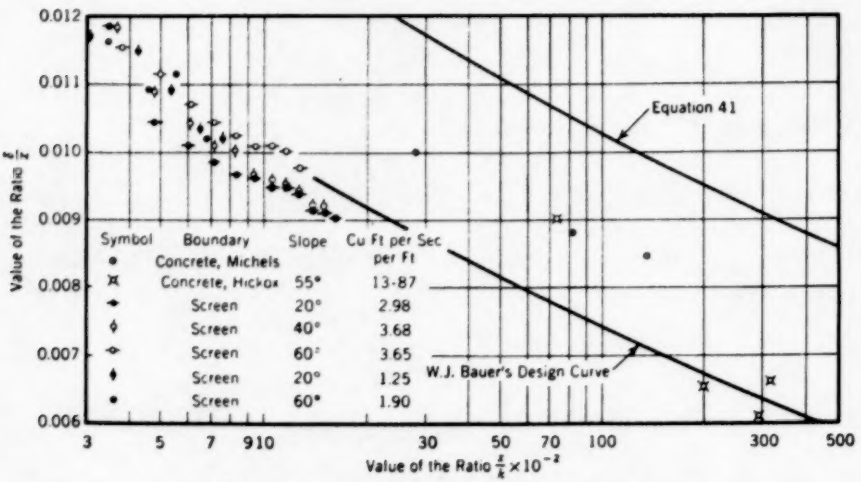

FIG. 17.—THE RATIO $\frac{\delta}{x}$ AS A FUNCTION OF THE RELATIVE ROUGHNESS FOR ROUGH BOUNDARIES

Mr. Hickox's data. However, it is noticeable that the measured values are larger than the computed ones. This is because the measured values account for the corrugation of the surface at the critical point.

It is also true that the Manning coefficient for concrete can be expected to be between 0.013 and 0.016, corresponding approximately to 0.004 ft $< k <$ 0.016 ft. A change in the value of k which is used to plot the points in Fig. 17 results

[17] "The Mechanics of Turbulent Flow," by Boris A. Bakhmeteff, Princeton University Press, Princeton, N. J., 1936, p. 90.

[18] "Some Prototype Observations of Air Entrained Flow," by V. Michels and M. Lovely, *Proceedings*, Minnesota International Hydraulics Convention, Minneapolis, Minn., 1953, p. 403.

in a constant translation parallel to the abscissa. For these reasons, it can be concluded that, whereas the general trend of the design curve is known, its position is not accurately determined.

From Eq. 34 it can be seen that

$$\frac{d\delta}{dx} = \frac{0.0074}{S^{0.1}} x^{-0.3} \quad \ldots\ldots\ldots\ldots\ldots\ldots\ldots\ldots (43)$$

For x equal to 10 ft, $d\delta/dx$ equals 0.0037. The divergence of the boundary layer is then 0° 13′. In the same manner, from Eq. 42,

$$\frac{d\delta}{dx} = 0.0378 \left(\frac{k}{x}\right)^{0.154} \quad \ldots\ldots\ldots\ldots\ldots\ldots\ldots\ldots (44)$$

For k/x equal to 0.0005, the divergence is 0° 40′. These low values for the divergence help one to understand why velocity distributions, valid in uniform flow, can also be applied to this case.

Mr. Bauer presents the experimental data on a physically sound basis. The data allow comparison with the results of a theoretical method of approach which was previously developed.[15] It is therefore possible to conclude that this method is accurate enough to predict the development of the boundary layer on smooth spillways. On rough spillways, it remains a difficult problem to decide which value of roughness to select. This problem, however, is not confined merely to this case; it will be solved when the mechanism of turbulent flow on rough boundaries is clearly understood. Fortunately, as pointed out by the author and as shown in Fig. 14, a large variation of k has little influence on the boundary-layer thickness. This circumstance enables the solution of design problems by the method described by Mr. Bauer.

William J. Bauer,[19] J. M. ASCE.—An able analytical appraisal of the writer's data has been made by Mr. Halbronn. Based on the needs of the researcher rather than the practicing engineer or designer, his discussion is an excellent example of how valuable sidelights can be derived from the laboratory data. In general, Mr. Halbronn's findings support the conclusions.

Mr. Halbronn has developed two expressions (Eqs. 29 and 31) for δ/x as a function of the Reynolds number $\mathbf{R}_x$. Essentially, Eq. 29 is based on the assumption of velocity distribution of the form of Eq. 33, and Eq. 31 is based on one of the forms given in Eq. 32. Testing the hypotheses thus developed in the light of the data shown in Fig. 13, Mr. Halbronn concludes that an expression similar to Eq. 32 better approximates the shape of the velocity profile. It is felt, however, that the actual shape of the velocity profile within a turbulent boundary layer cannot be accurately approximated by simple mathematical expressions of the types considered (Eq. 32 and Eq. 33), except over specified limited ranges of the Reynolds number. It should be noted that in Figs. 2 and 3 there is a consistent deviation (however slight) of the experimental points from the straight line which represents an expression of the form of Eq. 32. The deviation increases with increased values of the Reynolds

[19] Senior Designer, Harza Eng. Co., Chicago, Ill.

number, demonstrating the inadequacy (in this range of the Reynolds number) of the simple mathematical approximation.

Mr. Halbronn notes that in Fig. 2 the value of the exponent j of Eq. 32 would be 1/7.5. Actually, j in Fig. 2 decreases gradually as the Reynolds number increases, varying between 1/7.3 and 1/8. Similar trends were observed in the remainder of the data which were not published. Mr. Schlichting states[6] that beyond the range of validity of the Blasius law (the 1/7-power expression) "* * * a better approximation is obtained by the power 1/8, 1/9, or 1/10 instead of 1/7." The experimental data seem to confirm Mr. Schlichting's observation.

In analyzing the data for c_f, Mr. Halbronn has assumed a 1/7-power velocity distribution and has derived Eq. 36, an expression for c_f in terms of $\mathbf{R}_\delta$. On the basis of the previous comments, it is of interest to repeat the procedure for an 1/8-power velocity distribution. This procedure results in

$$c_f = 0.0427\, \mathbf{R}_\delta^{-2/9} \qquad (45)$$

The curve for Eq. 45 lies about as far above the data in Fig. 15 as Eq. 36 lies below, showing that the best fit would be associated with a value for j of between 1/7 and 1/8. This fit agrees with the previous indications as the observed values of j are between 1/7.3 and 1/8. It can be concluded, therefore, that the lack of agreement between Eq. 36 and the data is not caused by the inappropriateness of the form of the equation which has been used to approximate the velocity distribution, but rather to the use of an inappropriate value of j.

The excellent agreement between the data and Eq. 16 is surprising, as Mr. Halbronn has indicated, as this equation is based on the apparently inappropriate logarithmic velocity distribution. It is believed that this agreement is merely coincidental. The apparent agreement between the data and Eq. 31 in Fig. 13 is also somewhat coincidental as Eq. 31 is based on a slightly erroneous value of j, whereas the definition of δ in Fig. 13 does not agree exactly with the definition of δ used to derive Eq. 31. These two approximations have apparently tended to compensate for each other.

A misunderstanding has arisen concerning the significance of Fig. 10(a). Mr. Halbronn has suggested that the error lies in a mislabeling of the logarithmic abscissa scale. Actually, the proper abscissa scale for Fig. 10(a) ranges between 3×10^6 and 5×10^7 and is the value of $\mathbf{R}_x = U\,x/\nu$ and not $\mathbf{R}_{\delta m} = U\,\delta_m/\nu$. What the writer failed to explain was that Eq. 16 was first modified by a substitution of

$$\mathbf{R}_{\delta m} = f(\mathbf{R}_x) \qquad (46)$$

and then plotted in Fig. 10(a). Eq. 46 was determined from experimental data[20] (not published herewith).

In order to analyze the development on the rough bottom, Mr. Halbronn used the von Kármán-Prandtl velocity-distribution equations for uniform flow

[20] "The Development of the Turbulent Boundary Layer on Steep Slopes," by William J. Bauer, dissertation presented to the State Univ. of Iowa, at Iowa City, Iowa, in August, 1951, in partial fulfilment of the requirements for the degree of Doctor of Philosophy.

in pipe. Using Eq. 3 and Eq. 5 for the rough pipe (and making several necessary assumptions), he derived an expression for δ as a function of x and k, plotting it in Fig. 14 for three fixed values of k. Inasmuch as the assumed logarithmic velocity distribution is even further from the truth in the case of rough boundaries than in the case of smooth boundaries, the subsequent analytical results are of questionable value. In Fig. 3 are illustrated velocity profiles approximated by equations of the type of Eq. 32 wherein j ranges between 1/4.23 and 1/4.86. These values are far from the 1/7-exponent and 1/8-exponent which give better (yet inadequate) agreement with the logarithmic distribution.

The writer is pleased with the insertion of additional prototype data into Fig. 17, as well as with the tabulated comparison between measured and computed values of δ on the Glennmaggie Dam. It is agreed that the position of the design curve in Fig. 17 is not accurately determined (k remains in doubt). It should be noted (as Mr. Halbronn noted) that the range of doubt is sufficiently small to permit solution of design problems by the method illustrated in Fig. 11. Conservatism would merely indicate the assumption of a reasonably large value for k.

Discussion of
"AN EXPERIMENTAL INVESTIGATION AND LIMIT ANALYSIS OF NET AREA IN TENSION"

By W. G. Brady and D. C. Drucker
(Proc. Sep. 296)

W. H. MUNSE,[1] A.M. ASCE.—It is gratifying to see a new approach applied to a problem which the engineering profession has been studying for many years—that of determining the net area of a tension member. The writer, however, hopes that the analysis and tests presented in the paper by Messrs. Brady and Drucker will not be considered as the answer but only as a part of the answer or a starting point upon which it may be possible some day to build a better answer than is now available. These tests, as well as many of the previous tests on net section, have been conducted on flat-plate specimens and then analyzed in terms of design rules which are used for riveted or bolted connections in which the load transfer may differ greatly from that of the flat plate. The engineers need an accurate analysis or analyses for the behavior of tension members but will want assurance that the theory is applicable to realistic members.

The limit load theorems presented in this paper provide a new viewpoint insofar as the behavior of tension members is concerned. Consequently, it would have been helpful if the tests had been carried to failure and the relationships between the limit load and ultimate load-carrying capacity of the plates determined. This information would have made it possible to compare, at least in part, the result of these tests with the many tests reported in the literature.

In some structures, general yielding across an entire member may produce failure of the member or, at least, exceed its limit of serviceability; in other instances initial yielding or possibly, ultimate load-carrying capacity may be the limiting factor of serviceability and a more reasonable value upon which to base the working load. Thus, if the material is to be used efficiently, the mode of failure must be considered in any determination of working stresses and not only the limit load.

Consider, for example, a long tension member in a bridge. When general yielding occurs in the connections of such a member, this yielding is usually restricted to the first row of fasteners in the connections at either end of the member: a relatively small portion of the member. The effect of this plastic deformation in the connections on the overall deformation of the entire member may be small and have little effect upon the usefulness of the member; in all probability, it would be a general yielding of the entire member which would be the limiting factor for such a structure rather than the yielding at the connections. However, even after the entire member has been subjected to a general yielding, the member would still retain a considerable amount of additional load-carrying capacity.

In recent tests conducted at the University of Illinois on 18 in. I-sections

1. Research Associate, Prof. of Civ. Eng., Univ. of Illinois, Urbana, Ill.

with 1/2-in. gusset plates, it was found that the distribution of load in the members was greatly different from that generally obtained in flat plates. This results from the fact that the load is taken out of the member through only the flanges while a large percentage of the area of the members is concentrated in the web. However, strain measurements on the webs of the members provided data which can be correlated with the limit analysis study by the authors. A general indication of the behavior of the members may be obtained from the following tabulation.

Loading Conditions	Average Gross Stress, psi
Initial Yielding	15,000
General Yielding in Joint (Critical Section)	36,400
General Yielding in Gross Section	37,600
Ultimate Strength of Member	50,200

From the test data, it was found that general yielding in the joint (when the yield point strain was attained in the center of the web) occurred when the stress ratio T^*/T_0 or yield-strength efficiency for the member was 97 percent. However, the members failed at a test efficiency of approximately 74.5 percent. It appears that parts of the section may have been strained into the work-hardening range when the center of the web at the critical section reached the yield point strain. These data suggest that several analyses may be necessary to explain completely the behavior of tension members: an elastic analysis, a limit analysis, and an empirical ultimate strength relationship.

It is realized that the above discussion raises questions concerning the applicability of limit analysis to tension members. Nevertheless, the writer hopes that the authors will find it possible to pursue their study further and to expand it to include actual joints of various types as well as such other factors as variations in, pitch, gage, material properties, and the preparation of the fastener holes. By determining, in such tests, the limit loads as well as ultimate load-carrying capacity it may be possible to evaluate this information in terms of the limit analysis theorems as well as other concepts based on the ultimate strength or elastic properties of the materials.

P. P. BIJLAARD,[2] M. ASCE.—Calculations similar to those made by the authors, were published in Dutch by the writer in 1931, using the maximum shear stress yield criterion,[3] as well as the Mises criterion.[4] These calculations covered the subject more in detail than the authors did. A summary in English was given in a footnote on page 35 of reference 5. In addition to the calculations the writer made elaborate experiments.[3] Since both references 3 and 4 are in Dutch, the principal results will be given below. It will be shown in which situations the authors obtained essentially the same results as those of the writer's earlier investigations, and in which cases the two differ.

2. Prof. of Structural Eng., Cornell Univ., Ithaca, N. Y.
3. "Resistance of a section of a plate between rivets in an oblique row, calculated from the Mohr criterion of plasticity" (in Dutch), by P. P. Bijlaard, de Ingenieur (the Hague, Holland), Vol. 46, 1931, pp. B.47-B.57.
4. "Resistance of a weakened oblique section of a plate subjected to tension, calculated by the plasticity criterion of Huber-Hencky" (in Dutch), by P. P. Bijlaard, de Ingenieur (the Hague, Holland), Vol. 46, 1931, pp. B.249-B.251.
5. "Theory of local plastic deformations", by P. P. Bijlaard, Publ. International Association for Bridge and Structural Engineering, Vol. 6, 1940-41, pp. 27-44.

The writer showed that minor plastic deformations in a weakened section (AB in Fig. 1 of ABB^1A^1 in Fig. 3) result in a state of stress which produces maximum resistance against deformation before the section fails. This assumes an elasto-plastic stress-strain diagram of the mild steel type. This situation applies if the maximum shear stress yield criterion is used and, at the same time, plastic deformation is assumed to occur by sliding along the planes of maximum shear stress.[3] It also applies if the Mises criterion is used and, at the same time, plastic deformation is assumed to occur quasi-isotropically, that is, in the same way as the elastic deformation, but with a varying plastic modulus and with a Poisson's ratio of one half.[4,5]

If the maximum shear stress criterion is used for an oblique section like that of Fig. 1, one obtains a limit curve for the total stress $\mu = \sqrt{\sigma^2 + \tau^2}$ which is given by Fig. 2 for any angle α. For $\alpha = 0$ the total stress is $\mu = \sigma = \sigma_{ys} = 2k$, where σ_{ys} is the yield stress in tension and k is the yield stress in pure shear. The limit curve consists of a quarter circle with its center at $\sigma = k$ for $\alpha \leq 45^0$ and a straight line $\tau = k$ for $\alpha \geq 45^0$. For $\alpha \geq 45^0$ the state of stress in the oblique section AB at the limit load is given by a circle that touches the line PN at the end point Q of the pertinent vector μ_{AB} which represents the total stress μ on the weakened section AB (Fig. 2). On the other hand, the pure tensile stress assumed by the authors in obtaining their Equation (15) for $\alpha \geq 45^0$ would lead to a limit curve given by the dashed quarter circle NO which results in much lower limit loads than the limit curve PN.

At the same time[3] the writer showed that, if the plate is subjected to tensile forces P, subsequent to fully plastic deformation in the section AB, the relative movement of the elastic part of the plate below AB with respect to that above AB is given by the dashed arrow D, denoted as the direction of yielding. For $\alpha < 45^0$ as in Fig. 1, where the planes of maximum shear stress are not perpendicular to the middle plane of the plate, the arrow D subtends an angle $\omega = \alpha$ with the axis of the plate. If $\alpha \geq 45^0$ the planes of maximum shear stress are perpendicular to the middle plane of the plate, so that the direction of yielding coincides with AB, and $\omega = 90^0 - \alpha$.

In a symmetrical case, as in Fig. 3, it is not necessary that the forces F, transferred by the oblique sections AB and A^1B^1, are in the direction of the total force P, acting in the axis of the plate. If the forces F deviate by an angle γ from the axis of the plate, they will subtend angles $\alpha - \gamma$ with the normals to the sections AB and A^1B^1. Then, from Fig. 4, the total stress μ in AB and A^1B^1 is given by the vector OR and the effective stress in the direction of the force P by $\mu_e = \mu \cos \gamma$ (Fig. 3), given in Fig. 4 by the vector OS. It follows directly from Fig. 4 that $\mu_e = OS$ will be as large as possible if the perpendicular RS to OS is tangent to the limit curve MNP. In that case CR is parallel to OS and the angle $MOR = \alpha - \gamma = \alpha/2$, so that also $\gamma = \alpha/2$. Hence the limit curve for the effective stress μ_e for symmetrical sections is given by the locus MSP of the feet S of the perpendiculars RS, which was denoted as the pedal curve to the curve MNP. From Fig. 4 $\mu_e = k(1 + \cos \alpha)$ (reference 2, page B.54), so that the maximum force which a section AB or A^1B^1 in Fig. 3 can take is

$$P/2 = k\,t\,L\,(1 + \cos \alpha) \qquad (1)$$

where L = length, t = thickness.
The author's Equation (31) is identical with this equation, since their angle α is the complement of the writer's angle α.

Comparison of Figs. 1 and 3 shows why the forces F, acting on each of the

sections AB and A^1B^1, will establish themselves in such a way that $\gamma = \alpha/2$. In that case the forces F subtend angles $\alpha - \gamma = \alpha/2$ with the normals to the sections AB and A^1B^1. Hence from Fig. 1 the directions of yielding D will subtend angles $\omega = \alpha/2$ with the forces F, so that from Fig. 3 the vectors D are parallel to the axis of the plate. It is obvious that the directions D must be parallel to each other, since the elastic lower part of the plate in Fig. 3 moves in one direction only. Further, from symmetry, D must be parallel to the axis of the plate.

The case of the plate between oblique rows of holes is somewhat more intricate, since one has to determine which section between the holes will fail at the smallest limit load F (Fig. 5). In Fig. 2, the limiting total stress μ for a single oblique section is bounded by the curve MNP. The oblique sections which can take the same limit load as a normal section AA^1 (normal to the force F), with cross section A, must have cross sections $2\,k\,A/\mu$. Using μ from Fig. 2 it follows that all those equivalent oblique sections through a point (Fig. 5) are bounded by the curve ANA^1N^1, consisting of 2 straight lines of lengths equal to AA^1 and two semi circles with diameters equal to AA^1. For example, any oblique section LL, subtending an angle α with the section AA^1, which is normal to the force F, has the same limit load as the section AA^1. Consequently that section LL between the holes which can take the smallest load is obtained by placing the limit curve ANA^1N^1, using an appropriate scale, between the holes, so that it touches the perimeters of the holes. Then the section connecting the two tangent points, like LL in Fig. 5, is the weakest section. It was shown in reference 2 that the line LL must be straight. Hence in Fig. 5 the limit load for the section between the holes is equal to the limit load for the normal section AA^1, or equal to $2\,k\,(AA^1)\,t$, where t is the plate thickness.

For small values of β the holes will touch the straight parts of the limit curve ANA^1N^1, so that then, with the present notations (Equation (1) of reference 1),

$$AA^1 = \ell \cos\beta - d \tag{2}$$

For larger angles β the holes touch the circular parts of the limit curve ANA^1N^1, so that (Equation (2) of reference 1)

$$AA^1 = \frac{\ell^2 - d^2}{2(s + d)} = \frac{s^2 + g^2 - d^2}{2\,(s + d)} \tag{3}$$

Assuming, for purposes of design, the load F to be uniformly distributed over the section MM, in the line connecting the centers of the holes, the total limit stress μ_{mu} (in the direction of F) on this section would be

$$\mu_{mu} = \left[(AA^1)/(MM)\right]\ 2\,k \tag{4}$$

The limit curve for the oblique limit stress μ_{mu} is given graphically in Fig. 6 for the most unfavorable case when ℓ/d is as small as possible, which was assumed to be $\ell/d = 3$. This curve was denoted as the upper limit curve, since it was obtained, as shown above, by assuming the stress distribution in all planes to be as favorable as possible. Obviously these most favorable stress distributions differ for adjacent sections, so that they cannot always occur simultaneously.

In order to find a lower limit curve for several angles β (Fig. 5) a body of

equal plastic resistance was drawn between the holes, also assuming $\ell/d = 3$. This body was given such a form that practically everywhere within that body the state of stress, α_1, α_2, was at the yield stress, and such that the resistance of its effective section AB to the forces F was as large as possible (Fig. 7). The stress is uniformly distributed over this section AB, which subtends an angle $\alpha = \beta + \delta$ with the normal to the line of action of the forces F. In Fig. 7 the angle $\beta + \delta$ is chosen as $\tan^{-1} 2.5$, so that from Fig. 2, where μ_{AB} is the total limit stress on AB, the principal stresses are $\sigma_1 = 0.7\ \sigma_{ys}$, $\sigma_2 = -0.3\ \sigma_{ys}$. Fig. 7 speaks for itself. The load F that can be transferred between the holes is $F = (AB)\, t\, \mu_{AB}$, so that the stress $\mu_{m\ell}$, assumed to be uniformly distributed over the section MM = $(\ell - d)\, t$ (Fig. 5), is (Equation (7) of reference 1)

$$\mu_{m\ell} = \left[(AB)/(MM)\right] \mu_{AB} = \frac{2\, a\sqrt{2}}{\ell - d}\ \mu_{AB} \tag{5}$$

Since a more favorable stress distribution than that of Fig. 7 may be possible and since the material outside the body of equal resistance will restrain the plastic deformation, the stresses $\mu_{m\ell}$ determine a lower bound for the stress μ_m. By considering sections between holes for various angles β the limit curve in Fig. 6, denoted as lower limit curve, for the stresses $\mu_{m\ell}$ was obtained.

In connection with the results of the writer's tests (single circles in Fig. 8) he assumed the upper limit curve to be a sufficiently accurate bound for the limit stress μ_m. The limit stress μ_{ms} of symmetrically situated sections is bounded by the pedal curve of this limit curve (Fig. 6).

The writer repeated the same investigation on the basis of the Mises criterion of plasticity.[4] This leads to limit curves for μ_m and μ_{ms} as shown in Fig. 8 (reference 4, page 35). The writer's test results with single and symmetrical oblique sections between holes are given by the single and double circles, respectively. Since the rotation of the forces F through an angle γ (compare Fig. 3) may overstress other sections and since it is too difficult to prescribe where the curve for μ_{ms} can be used and where not, in reference 4 the writer recommended the limit curve for μ_m for use for all sections. It is an ellipse with the equation

$$\sigma^2 + 3.3\tau^2 = \sigma_{ys}^2 \tag{6}$$

It leads to allowable total stresses in the section MM between the holes (Fig. 5) of (reference 4, Equation (18))

$$\mu_m = \frac{\sigma_{all}}{\sqrt{1 + 2.3 \sin^2 \beta}} \tag{7}$$

where σ_{all} is the allowable stress for pure tension, so that the allowable force F is (Fig. 5) $(MM)\, t\, \mu_m = (\ell - d)\, t\, \mu_m$.

The conditions used by the authors for obtaining the upper and lower limit loads are essentially identical to those used by the writer in reference 2 and lead to the same results. The reasons why the limit loads obtained by the authors are not as close together as those in reference 2 is that they did not consider the most unfavorable or the most favorable cases.

The writer does not agree with the authors that the $s^2/4g$ specification is

rather reasonable, since for a section subjected to pure shear, where g = 0, $s^2/4g$ would become infinite. Actually their Equation (33), which is based on their Equation (31), identical with the writer's Equation (1), and which equates $\sqrt{1 + s^2/b^2}$ to $1 + s^2/2b^2$, does not hold if s/b is more than approximately unity. If s/b is large, so that $\sqrt{1 + s^2/b^2}$ is about equal to s/b, from Eq. (33)

$$T_1^* = ktb \left[(s/b) + 1\right] \cong k\,t\,s$$

Actually for large angles β it is more unfavorable to consider the section MM between the holes (Fig. 9). If β becomes 90°, from Eq. (1)

$$F = k\,t\,L\,(1 + \cos\alpha) = k\,t\,L = k\,t\,(s-d)$$

so that the limit stress for $\beta = 90°$ is k, as also follows from Fig. 4. However the writer again wants to recommend Equation (7) for the allowable stress in the sections MM between the holes (Fig. 5), which, in terms of the pitch or stagger s and the gage g, may be written as

$$\mu_m = \frac{\sigma_{all}}{\sqrt{1 + 2.3\,\frac{s^2}{s^2 + g^2}}} \qquad (8)$$

and which he has used in design for about 25 years.

For more details the writer has to refer to his papers. In his theoretical investigations he assumed that the rivets do not keep the holes round, since they do not completely fill the holes, as is confirmed by tests done by others at that time and later.

W. G. BRADY[6] and D. C. DRUCKER, A.M. ASCE.[7]—The discussion by Professor Munse is a very helpful addition to the paper emphasizing as it does the limitations of limit analysis. In most, but not all, problems of importance in civil engineering first yielding or purely elastic action is not really of great significance. In most cases the limit load will be the maximum load which the engineer would wish to consider and so will base his factor of safety upon it. As Professor Munse points out, however, ultimate strength may be of more interest in many problems. As to the example of the I-beam loaded through the flanges only, it is likely that limit analysis will show an efficiency of the order of 75% rather than 100 because work hardening is not taken into account.

Professor Bijlaard's contributions to the theory of plasticity and its applications are well known and it is regretted that no reference was made to his papers on the effect of holes and notches. Their presentation in English is most welcome. Professor Bijlaard demonstrates the well known fact that an experienced engineer can obtain good answers to the most complicated problems. It should be noted, however, that the upper or lower bounds he describes are not necessarily either. The limit theorems as given in the paper

6. Cornell Aeronautical Laboratory, Inc., Buffalo, N. Y.
7. Prof. of Eng., Brown Univ., Providence, R. I.

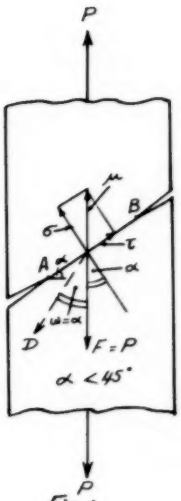

Fig. 1

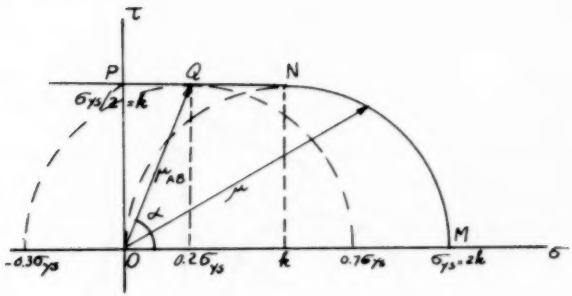

Fig. 2

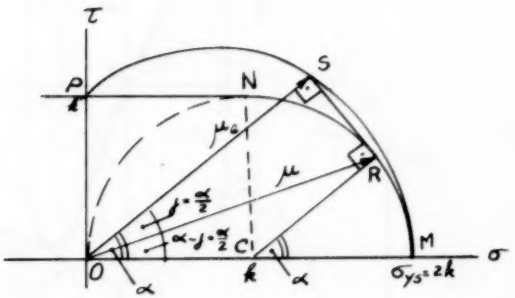

Fig. 4

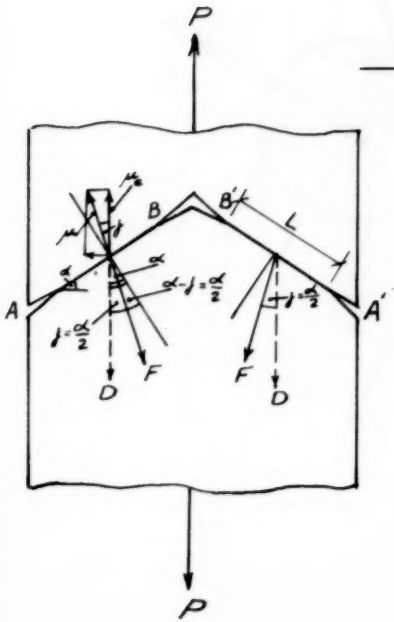

Fig. 3

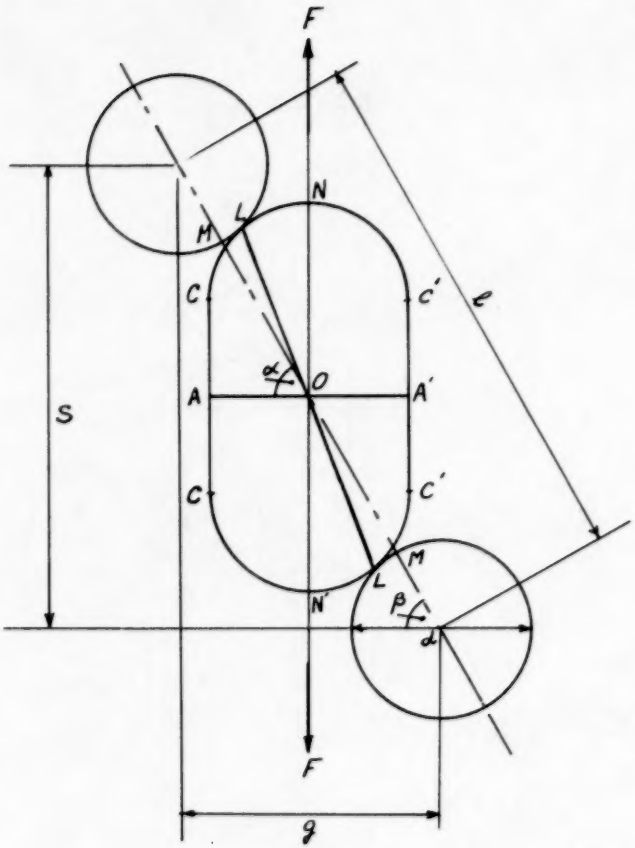

Fig. 5

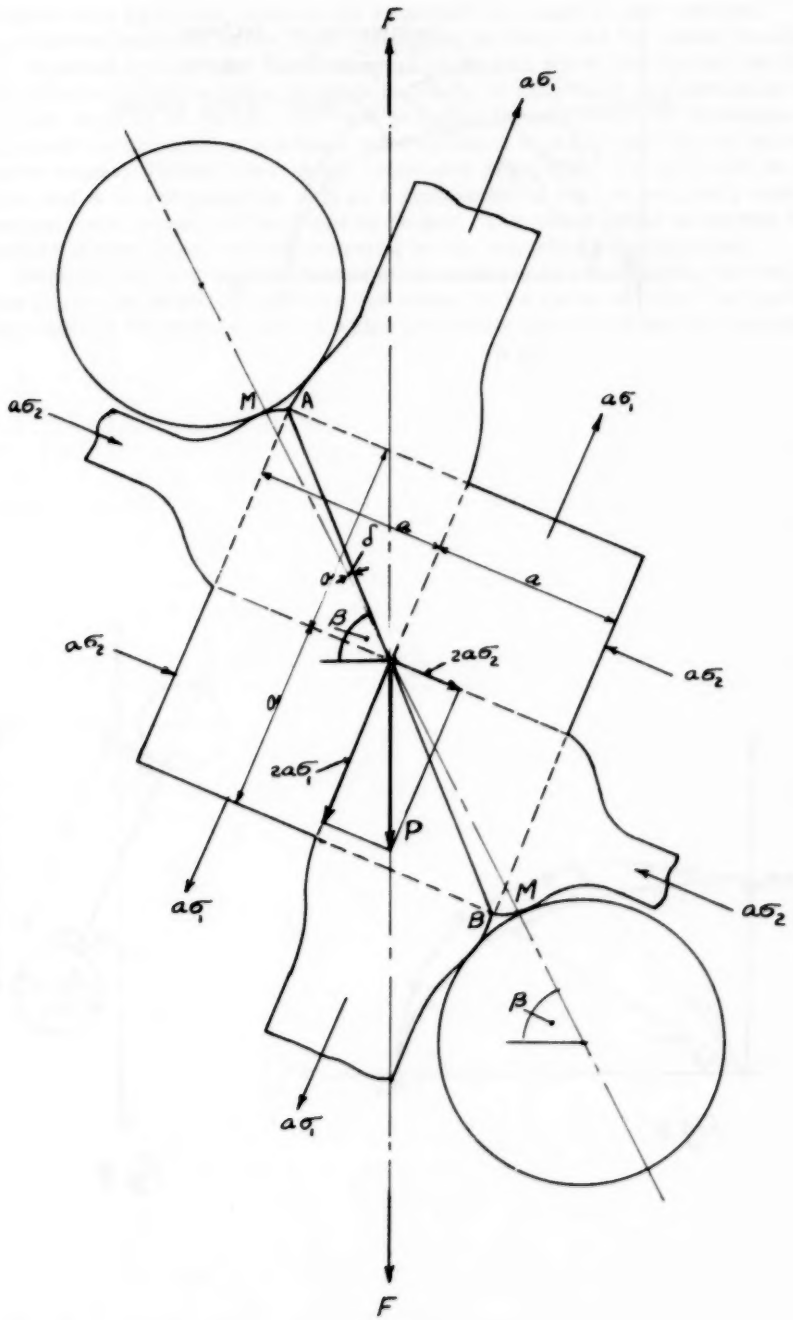

Fig. 7

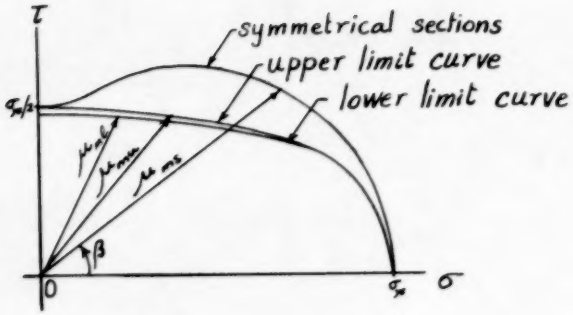

Fig 6

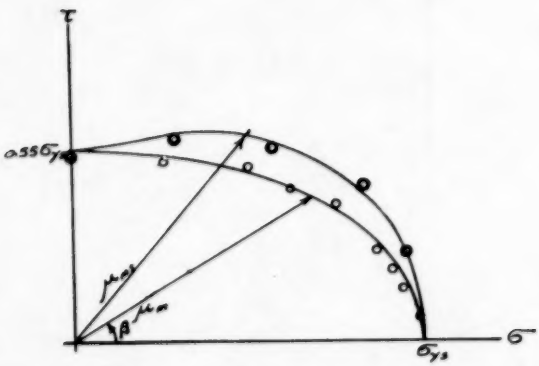

Fig. 8

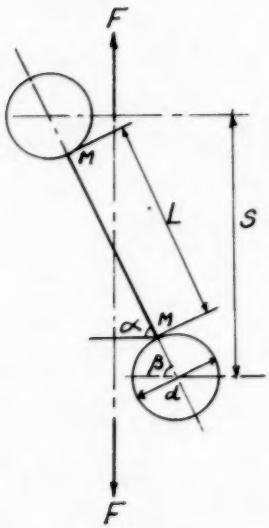

Fig. 9

require that kinematic patterns be employed for upper bounds and that equilibrium patterns below yield throughout be employed for lower bounds. As reported in the paper the theory and tests both show clearly that the number of rows of holes has a significant effect. A simplified discussion in terms of what happens in the two row case is not sufficient. Fig. 7 of Professor Bijlaard's discussion would have to be extended to the boundaries of the sheet under tension without altering the calculated axial pull. The difficulty in doing this, and it is a physical as well as a mathematical one, is precisely what causes lower bounds in the paper to be low. The added effort to narrow the bounds is very great and not essential in the majority of applications.

Perhaps the real contribution of limit analysis is not in aiding the engineer who knows the practical answers but rather in its value as a tool for the inexperienced to produce results which otherwise take a lifetime of learning.

Discussion of
"DESIGNING ALUMINUM ALLOY MEMBERS FOR COMBINED END LOAD AND BENDING"

By H. N. Hill, E. C. Hartmann, and J. W. Clark
(Proc. Sep. 300)

HERBERT A. SAWYER, JR.,[1] A.M. ASCE.—Certain important refinements to present practice in designing beam-columns have been presented in this paper, these refinements applying not only to aluminum members, which were exclusively considered by the authors, but, as the authors hint and as the writer believes, to members of other structural materials as well.

The authors present evidence and conclude that interaction Eq. 9 gives a reasonably accurate, simple means for calculating the strength of aluminum alloy beam-columns. The authors' justification of this equation for failures by bending in the plane of the applied bending moment was entirely empirical, and therefore they carefully state that additional investigative work is needed to determine the limits of this equation's applicability for conditions differing from those of the cited tests. The cited tests were restricted to (1) aluminum alloy members with (2) applied bending constant throughout length and with (3) applied bending stresses less than half of the ultimate bending modulus ($f_b < f_B/2$).

The purpose of this discussion is to consider certain theoretical and experimental evidence on the use of this equation outside of these restrictions.

Theoretical Evidence

The writer has previously derived[2] an expression for the strength of beam-columns very similar to Eq. 9:

$$\frac{f_c}{f_{CO}} + \frac{f_b}{f_B\left(1 - f_c/f'_{CE}\right)}\left(1 + K f_c/f'_{CE}\right) = 1 \qquad [12]$$

where f_{CO} = strength per unit area of a short column.

$f'_{CE} = \frac{\pi^2 E_t}{(L/r)^2}$ where E_t is the tangent modulus of the material at a stress of f_c (not f_C).

K = a constant which depends on the distribution of the applied moments, that is, the distribution of either initial eccentricities or initial moments from transverse loads; for triangular distribution equal to about -0.18, for sinusoidal 0.00, for parabolic +0.03, for third-point trapezoidal +0.05, for quarter-point trapezoidal +0.13, and for rectangular about +0.26.

1. Assoc. Prof. of Civ. Eng., Univ. of Connecticut, Storrs, Conn.
2. "Applied Column Theory" by F. R. Shanley, discussion by H. A. Sawyer, Transactions ASCE, Vol. 115, 1950, p. 743, Eq. 71.

This equation was derived from the basic column equation, $f = P/A - Mc/I$, using a generalized secant-formula type of derivation and assigning to "f" a sliding, limiting value varying from the short column strength for concentric loadings to the modulus of bending (or rupture) for pure bending loadings. Of course the main theoretical limitation of Eq. 12 is its inaccuracy above the elastic limit; the use of E_t instead of the elastic modulus somewhat reduces this inaccuracy. Another limitation of Eq. 12 is that it applies only to failures from bending in the plane of the applied moment. However, this is the case for which the authors gave only empirical justification for Eq. 9. The following comparison of Eqs. 9 and 12 is made to reveal certain theoretical justifications and limitations for this case of Eq. 9.

The factor containing K of Eq. 12 is significant in giving what the writer believes to be a fairly correct indication of the relative adjustments which should be made in the bending term of Eq. 9 to account for distributions of applied moment which are not of the rectangular shape considered in this paper. For example, to take the most extreme case, if the primary bending of a beam-column is caused by a single transverse load at the mid-length (or out-of-lineness caused by a single short bend of the axis at the mid-length) the primary moments would be triangular in distribution, and according to Eq. 12 the bending term of Eq. 9 should be multiplied by the factor:

$$\frac{1 - 0.18 \frac{f_c}{f'_{CE}}}{1 + 0.26 \frac{f_c}{f'_{CE}}}$$

However, the importance of this factor should not be overestimated; it differs from unity significantly only when the term f_c/f'_{CE} is relatively large, but for large values of f_c the bending term of the interaction equation is relatively small and insignificant, and large percentage variations of this small term will have little effect on the allowable axial load. Therefore, for most design purposes the omission of this variation in Eq. 9 is justified, especially since this omission is always on the safe side.

The remaining differences between Eqs. 9 and 12 are also more apparent than real. The term f'_{CE} differs from f_{CE} only for large values of f_c, but for such values the bending term of the interaction equation is relatively small. This difference tends to make Eq. 9 slightly less conservative than Eq. 12. The remaining difference, that between f_C and f_{CO}, disappears for low values of L/r and is unimportant for low values of f_c, but for the higher values of L/r and f_c it becomes more significant, tending to make Eq. 9 more conservative than Eq. 12 in this range.

It may be concluded that with the exception of the range just mentioned Eq. 12 lends a sort of theoretical justification to Eq. 9 encouraging the expectation that Eq. 9 would apply for materials and loadings other than those of the cited tests.

Any designer attempting to use Eq. 9 (or Eq. 12) should note that the Euler-Engesser column equation which gives the basic column strength differs from the usual practical design formulas in that it neglects the effect of accidental eccentricity and heterogeneity. Also, the effect of accidental eccentricity was meticulously eliminated in the cited tests. Since such effects cannot be eliminated in practical construction, they always exist for both principal bending axes. The probable maximum accidental eccentricities must be predicted and

the resulting stresses included in the term f_b. Provision for accidental eccentricities by increasing the factor of safety of the Euler-Engesser formula is not satisfactory because eccentricity, and hence the percentage reduction in allowable load from eccentricity, tends to increase with increase in column length. For example, a standard out-of-lineness tolerance for aluminum alloy tubing is one-twelve-hundreth of its length.[4]

Experimental Evidence

The surest way to justify extension of the range of Eq. 9 is by comparison with test results. Messrs. Tuckerman, Petrenko, and Johnson[5] have performed extensive tests of steel and aluminum alloy tubing under combined axial and third-point transverse loads. The writer's Fig. 1 shows a comparison between these test results, Eq. 9, and Eq. 12 for tests of duralumin tubing. Eq. 9 conforms to these test results very well except for the highest values of L/r. This exception agrees with the conclusion of the above discussion. The writer believes that the disagreement for L/r = 30 may not be significant because the modulus of bending tends to increase for low values of L/r and such increases were neglected in the report of these tests. Note that Eq. 9 is on the side of safety for all values of L/r.

Chrome-molybdenum steel tubing was used for the remaining Tuckerman tests. The writer has shown elsewhere[6] the remarkable agreement between Eq. 12 and these tests. Eq. 9 may also be compared with these test results, and such comparison shows a good agreement for values of L/r from 30 to 70. As would be expected, Eq. 9 becomes conservative for higher values of L/r, the curve of Eq. 9 for L/r = 90 practically coinciding with most of the experimental curve for L/r = 100, and the curve of Eq. 9 for L/r = 120 practically coinciding with most of an extrapolated experimental curve for L/r = 140.

Conclusion

It may be tentatively concluded on the basis of these comparisons with theory and the Tuckerman test data that Eq. 9 may be applied with safety to certain beam-columns: (1) of some metals other than aluminum; (2) with applied bending moments from transverse loads, and (3) with applied bending stresses greater than half the bending modulus. Also, Eq. 9 is superior to Eq. 12 for general design purposes: it follows somewhat better, according to the writer's check, the aluminum alloy test data of the paper; its variation is generally on the safe side; and, most important, it is suitable for failures by "lateral" buckling (buckling about a bending axis perpendicular to the bending axis for the applied moment).

Lateral buckling neglected, the chrome-molybdenum-steel example and theoretical considerations would seem to indicate that Eq. 12 would prove

4. "Alcoa Structural Handbook," Aluminum Co. of America, Pittsburgh, Pa., 1945, p. 174.
5. "Strength of Tubing Under Combined Axial and Transverse Loading," by L. B. Tuckerman, S. N. Petrenko, and C. D. Johnson, Technical Note No. 307, National Advisory Committee for Aeronautics, Washington, D. C., June, 1929.
6. "Applied Column Theory" by F. R. Shanley, discussion by H. A. Sawyer, Transactions ASCE, Vol. 115, 1950, pp. 717, 744, Figs. 15, 23.

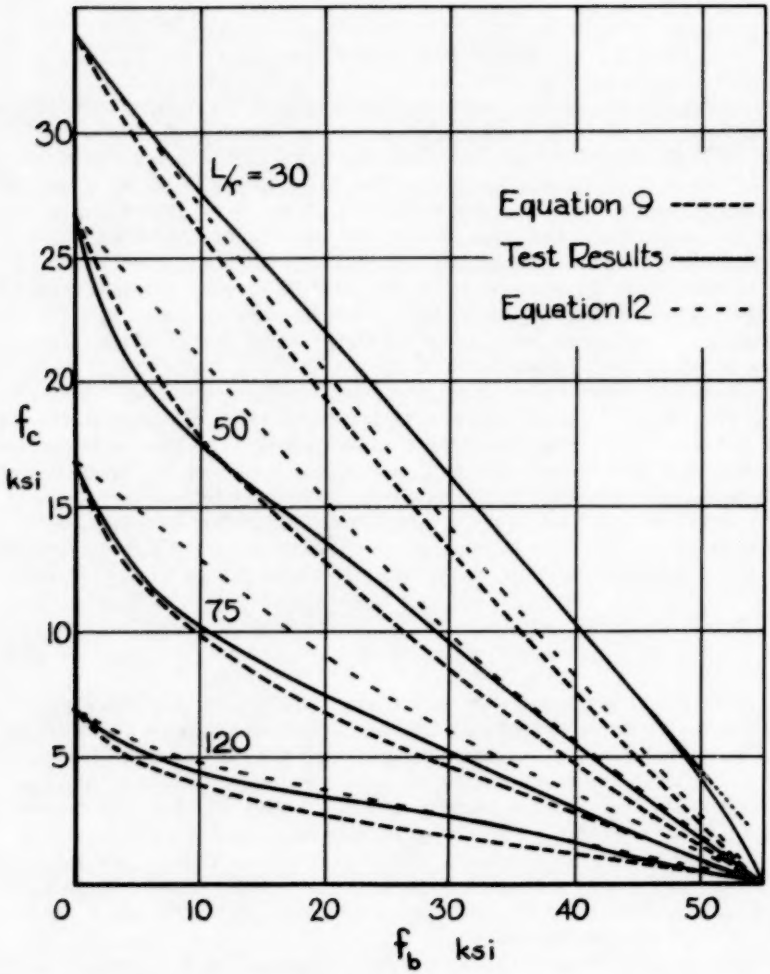

Sawyer on Hill et al, Fig. 1 -- Comparison of Tuckerman Tests of Dural Tubing, Eqs. 9, 12

more precise than Eq. 9 for materials such as mild and certain alloy steels, wood, and cast iron (with either sharp knees or somewhat uniform curvature in their stress-strain diagrams). However, on the basis of the presently available data, Eq. 9 seems to be the more generally applicable and safe, as well as being simple and suitable for design. The authors' Fig. 4 demonstrates the inadequacy of the conventional interaction formula for beam-columns. Therefore the authors of this paper have made a significant and valuable contribution to the art of structural design.

H. N. HILL,[7] M. ASCE, E. C. HARTMANN,[8] M. ASCE, and J. W. CLARK,[9] J.M. ASCE.—The discussers have made several interesting observations on the design of members for combined end load and bending. Mr. McCalley's equation (a) expresses the critical bending moment for the general case in which both the cross section of the member and the condition of loading are unsymmetrical. Equation (a) represents the same relationship as that derived by Goodier (reference 9, equation [9]), but Mr. McCalley has succeeded in stating the relationship in a manner that is particularly useful for design purposes. A special case that might be of interest is the case in which the cross section of the member is symmetrical but the loading is not; that is, the plane of the applied bending moment does not coincide with one of the principal axes. In this case "e" is zero and equation (a) reduces to the following:

$$M_{cr} = \frac{\pi}{KL}\sqrt{\frac{EI_1I_2GJ}{I_y}}\sqrt{1+\frac{\pi^2}{(KL)^2}\frac{EC_3}{GJ}}$$

It is worth noting that the value of the end fixity factor "K" in the foregoing equations always depends upon the restraint against rotation of the end cross sections about the minor principal axis, even though in the case of unsymmetrical bending the minor principal axis is not in the plane of the applied bending moment. Thus, the ends of a beam may be "fixed" in the lateral direction (normal to the plane of the applied bending moment) yet not fixed in the direction that is of interest from the standpoint of determining "K." This was demonstrated in a recent paper on the strength of aluminum alloy Z beams subjected to pure bending moment.[10]

It is gratifying that Professor Sawyer has furnished additional evidence in support of the use of equation (9) in the design of aluminum alloy beam-columns. His theoretical analysis of equations (12) and (9) supplements the discussion of interaction equations and their rational basis in section VII of the original paper.

Prof. Sawyer points out that the Euler-Engesser Column Formula does not include the effects of accidental eccentricity or heterogeneity, and he concludes, "Provision for accidental eccentricities by increasing the factor of safety of the Euler-Engesser formula is not satisfactory because eccentricity, and hence the percentage reduction in allowable load from eccentricity, tends to increase with increase in column length." It is true that initial crookedness

7. Asst. Chief, Eng. Design Div., Aluminum Co. of America, New Kensington, Pa.
8. Chief, Eng. Design Div., Aluminum Co. of America, New Kensington, Pa.
9. Research Engr., Aluminum Co. of America, New Kensington, Pa.
10. "Lateral Buckling of Channels and Z-Beams," by H. N. Hill, Proceedings, A.S.C.E., Separate No. 334, November, 1953.

tends to increase with increasing length of column; however, it does not follow that the factor of safety resulting from the use of a formula for ideal columns decreases for the longer columns. As a matter of fact, if eccentricity is directly proportional to length, the minimum factor of safety given by a formula for ideal columns occurs in the general vicinity of the juncture between the elastic and inelastic portions of the column curve.

The above statement is illustrated in Figs. 9 and 10. The solid curve in Fig. 9 is the Euler-tangent modulus column curve for aluminum alloy 61S-T6 rectangular tubes tested in the investigation described in reference 16. The lower, dashed curve in Fig. 9 represents the column strength calculated from equation (9) for the same specimens loaded as pin-ended columns with a ratio of eccentricity, "Δ", to length, "L," of 1/1200. None of the column specimens described in reference 16 had a "Δ/L" ratio of exactly 1/1200. However, test values of column strength corresponding to this ratio of eccentricity to length were found by interpolation from the test data. These interpolated test values are also plotted on Fig. 9.

Fig. 10 shows the ratio of column strength for a "Δ/L" of 1/1200 to the strength of an ideal column determined from the curves and test points in Fig. 9. Both the calculated curve and the test points in Fig. 10 illustrate the fact that the reduction in column strength caused by eccentricity does not necessarily increase with increasing length, even though the eccentricity itself does. Therefore, it does not appear unreasonable to design columns on the basis of formulas for ideal members, taking account of the effects of accidental eccentricity in the factor of safety.

April 16, 1954

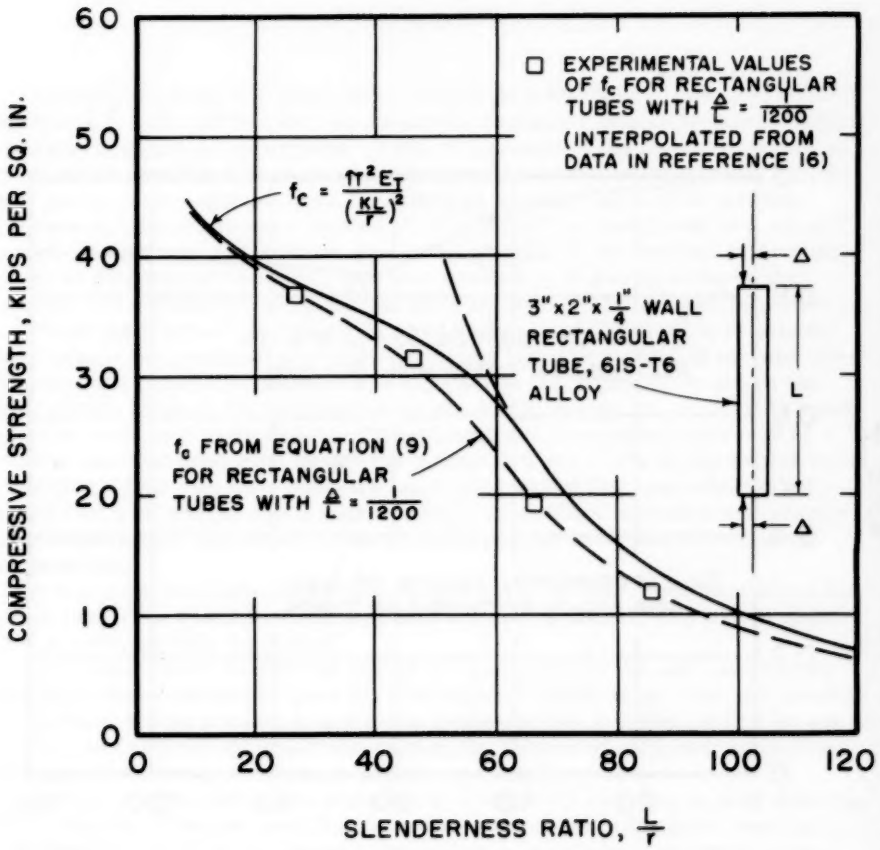

FIG. 9 - STRENGTH OF COLUMNS WITH $\frac{\Delta}{L} = \frac{1}{1200}$

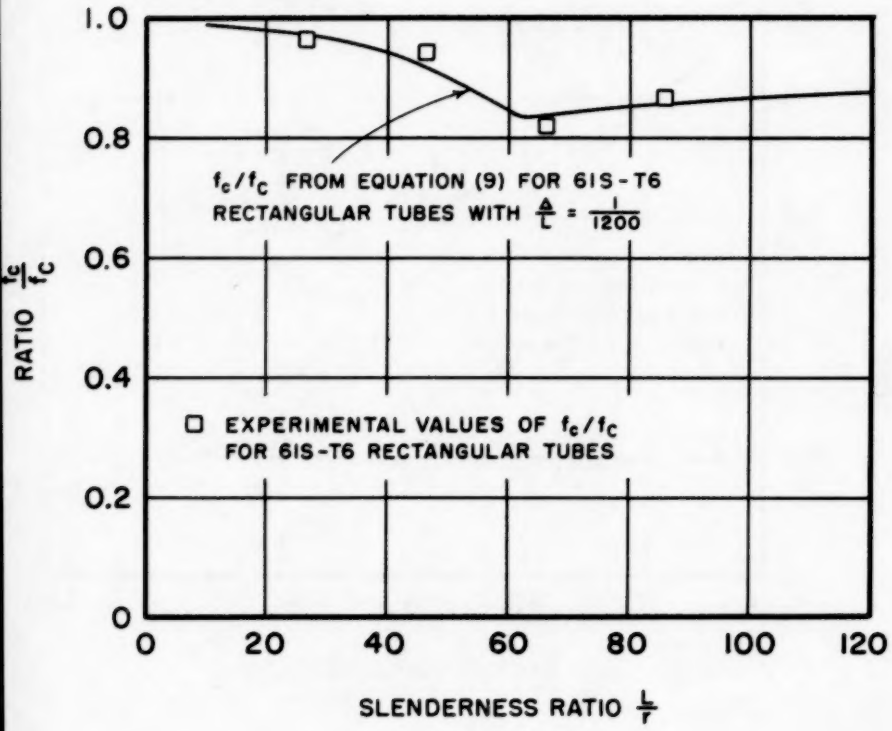

FIG. 10 - REDUCTION IN COLUMN STRENGTH WHEN $\frac{\Delta}{L} = \frac{1}{1200}$

Discussion of
"PLASTIC DEFORMATION OF WIDE-FLANGE BEAM-COLUMNS"

By Robert L. Ketter, Edmund L. Kaminsky, and Lynn S. Beedle
(Proc. Sep. 330)

ROBERT L. KETTER[1] J.M., and EDMUND L. KAMINSKY,[2] J.M., and LYNN S. BEEDLE,[3] A.M. ASCE.—The discussion by Professor Winter focuses attention on several points of importance. First of all, each of the members tested as part of the experimental study was loaded with a combination of axial thrust and end moments applied about the stronger principal axis of the section. Moreover knife edges were located at each end of the specimens in a manner which allowed rotation about an axis perpendicular to the web but restrained it in the direction of the web. This was done since it was considered that strong-axis bending is that condition most frequently encountered in practice.

From the previous Lehigh study cited by Professor Winter[4] it is possible to compare the predicted strength of columns with the results of pin-end tests in which the possibility of twist was eliminated. In Figure 42 is shown the correlation between the predicted strength curve (Figure 38, $ec/r^2 = 1.0$) and a set of weak axis tests (3I5.7). The collapse solution neglecting residual stress has been used even though the members were tested in the as-delivered condition. This was done since the pure axial test of the same section indicated that a relatively small amount of cooling residual stresses was present in the specimen. Agreement between the predicted and observed values is reasonable.

A few tests have now been made on columns of 8WF31 shape bent about the weak axis. The results will be included in a future report; they are in excellent agreement with the theory.

The second point raised was that of the generality of the assumed cooling residual stress pattern (Figure 7). Although the actual magnitude and pattern of residual stress present in any given cross-section is influenced by its geometric proportions, stresses observed in the flanges of column-type sections actually do not vary as much as might be expected.

In Figure 43 is plotted the distribution of residual stresses in four different WF columns. They indicate that the assumption made in the paper was not unreasonable. All of these shapes have compressive residual stresses at the flance edges. More recent measurements made on still other WF column shapes (12WF50, 12WF65, 6WF15.5, 14WF43) show a similar result.

Since the investigation is concerned with columns and not with beams, then shapes with flanges that are narrow in comparison with beam depth are not of prime interest. Further the 8WF31 shape is rolled in more tonnage than most

1. Research Asst., Lehigh Univ., Fritz Eng. Lab., Bethlehem, Pa.
2. Dept. of Civ. Eng., Syracuse Univ., Syracuse, N. Y.
3. Asst. to the Director, Lehigh Univ., Fritz Eng. Lab., Bethlehem, Pa.
4. Johnston, Bruce and Cheney, Lloyd, "STEEL COLUMNS OF ROLLED WIDE FLANGE SECTION", American Institute of Steel Construction, Progress Report #2, November, 1942.

other columns. Finally, since the flanges provide the majority of the bending stiffness, the magnitude and pattern of residual stress present in the web of the specimen is of relatively minor importance.

Professor Winter states, "The quoted test results seem to indicate that this feature, influence of twist, may prove to be of far greater consequence in reducing the strength of such members than the influence of residual stresses . . . .", such a separation of the influence of twist from that of residual stress may be misleading. Torsional stiffness is made up of essentially two parts: a St. Venant type of torsional stiffness and a cross-bending type. Discounting the first factor for the purposes of this discussion, (its influence will decrease as length decreases) the second factor, cross-bending stiffness, is markedly affected by residual stress. If, for example, a flange had yeilded due to residuals and applied stress to a distance equal to 1/4 of the width of the flange from each side, the cross-bending stiffness of that flange containing residuals would be 1/8 as large as for the same one without such initial stress imperfections. True, the inelastic lateral-torsional problem has not been solved and a solution is urgently needed, but this solution must include the influence of residuals if it is to solve the problem that is present in practice.

The final point concerns the correlation with the restrained column tests carried out at Cornell (see Figure 41). As was discovered independently both by the authors and the discusser, the implied application of the theory to this particular problem does not lead to the correct solution. Instead, the proper procedure is as follows:[5]

1. Given the spring constant, β_o, assume effective length for various P/P_y values.
2. Determine η from Figure 44 knowing P/P_y and cL/r.
   (Note: η is the secant to the $M/M_y - \phi / \phi_y$ curve at the point corresponding to collapse of the member in question. This information was available from the calculations leading up to Figures 37 and 38.)
3. Check "c" by using the Cornell β_o/η EK versus "c" curves.[6]
4. Repeat steps 1., 2., and 3. until the assumed "c" values agree with those calculated.
5. Using the correct "η" values corresponding to each assumed P/P_y, determine the relation between ϵ and e from Eq. 8 of the Cornell Report (ASCE Sep. 292).
6. Determine (P/P_y) and (ϵ/r) for the corresponding (cL/r) values from Figure 38 of this report.
7. Obtain e/r versus P/P_y by multiplying the results of steps 5. and 6.

The corrected curve is shown in Figure 45. It is in reasonable agreement both with the test results and with the Cornell analytical solution.

5. This procedure is a modification of one developed by Messrs.: Bijlaard, Fisher, and Winter and has been presented in more detail in the authors' discussion of ASCE Separate 292 (Vol. 79).
6. Winter, G., Hsu, P. T., Koo, B., and Loh, M. H., BUCKLING OF TRUSSES AND RIGID FRAMES, Cornell University, Engineering Experiment Station, Bulletin 36, April 1948.

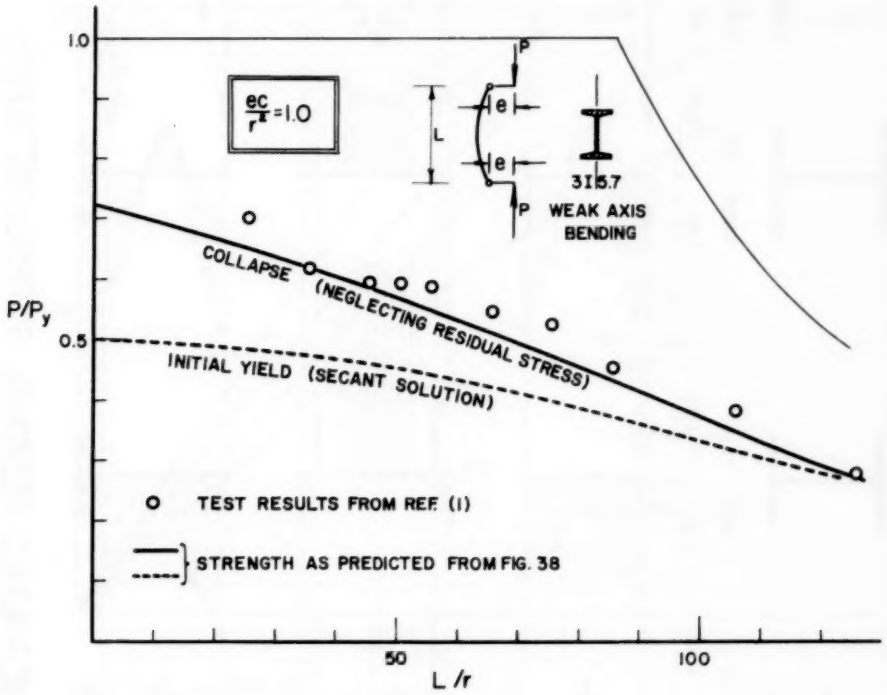

FIG 42 CORRELATION BETWEEN PREVIOUS LEHIGH TESTS (I) AND THEORETICAL COLLAPSE ANALYSIS

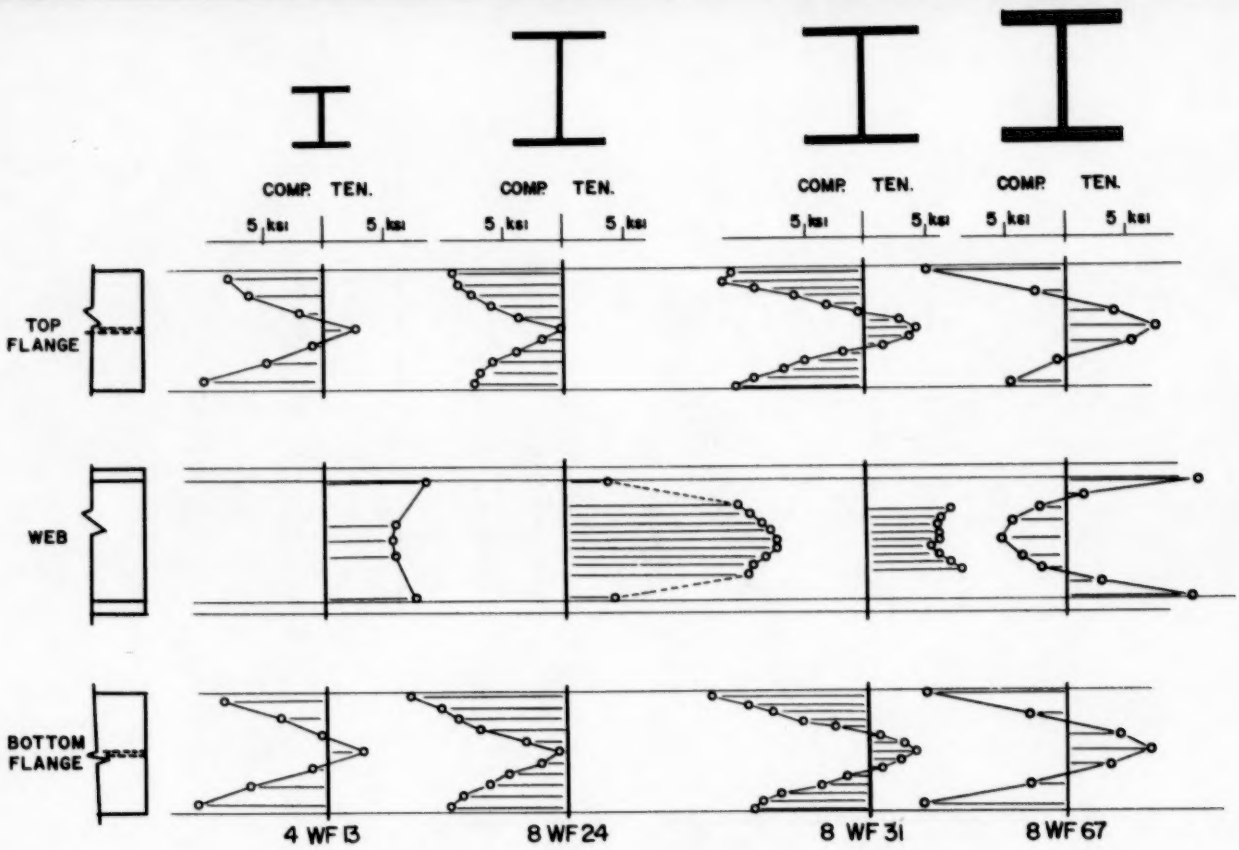

FIG 43 MEASURED RESIDUAL STRESS PATTERNS

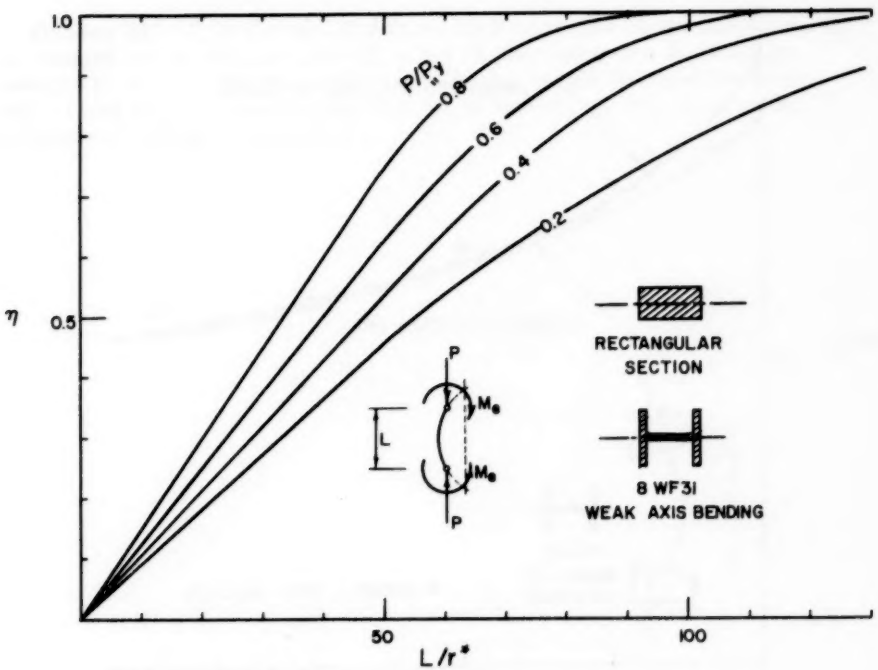

$L/r^* = (L/r)\sqrt{\sigma_y/40.0}$, σ_y in ksi

FIG. 44 PLASTIC REDUCTION FACTOR FOR 8 WF 31 SECTION, WEAK AXIS BENDING

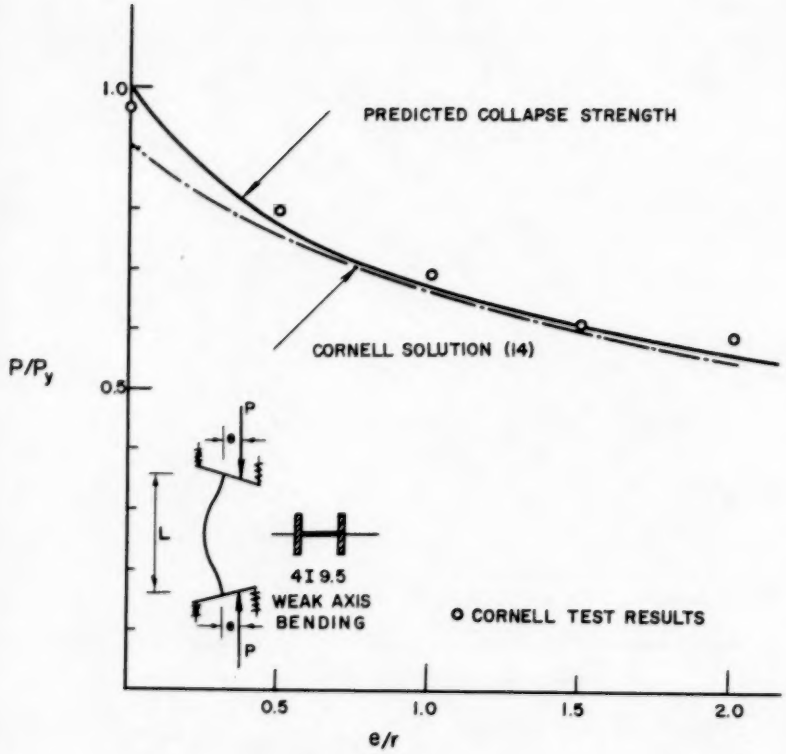

FIG. 45 CORRELATION BETWEEN CORNELL TEST RESULTS (14) AND THEORETICAL ANALYSIS FOR ANNEALED MEMBERS

CORRECTION TO DISCUSSION OF THE APPLICATION OF HEAVISIDE'S STEP-FUNCTION TO BEAM PROBLEMS

(Proc. Sep. 202)

On page 333-17, in the fifth line from the bottom, the coefficient 0_1 should be changed to C_1. On page 333-18, in Eq VI, the factor (x - 2) should be changed to (x - a). To the line following Eq VI, should be added the term: $+b_0$ k sen k (x - a). Also on page 333-18, in line 25, the last term within brackets should be a_0 instead of a.

Discussion of
"DEFLECTIONS OF A CIRCULAR BEAM OUT OF ITS INITIAL PLANE"

by Enrico Volterra
(Proc. Sep. 375)

I. OESTERBLOM,[3] M. ASCE.—In the English language, the subject of the paper was ably treated as early as 1914 by A. H. Gibson and E. G. Ritchie (22). Two distinguished authorities, Messrs. Pippard and Barrow, made extensive studies of and published papers and books on the arc bow girder (10) (11). One could ask for no more complete treatment of the theory of bow girder deflections and of the application of this theory. A book (23) which is a résumé of many years work has been published by Messrs. Pippard and Barrow. The German references are also extensive, but none that specifically refer to the subject or have usefulness in design was published earlier than the English works. Thus, one questions whether or not the paper advances new theories in the design or construction of civil engineering work, especially as the selected solutions do not include a graph for the almost universal case, $2\gamma = 180°$. Arc bow girders are usually supported at right angles to the structural frame and, when they are close to the frame (these are usually only ornamental in purpose), the designing engineer need not—and cannot afford to—spend time on extensive calculations. The author suggests (Fig. 1) five equidistant cuts of the circle, without explanation in the text, and develops three of them into helpful graphs. However, if wall wedges of 120° and 45° were common, the arc bow girders would be placed not at the point of the wedge but somewhere on the face of the wall so that 2γ would equal 180°.

Solutions to more comprehensive, varied, and real problems than those of this paper may be found in papers and books previously published. The author has referred to some that seem superior to his own presentation from the standpoint of the progress indicated and the utility shown. A bulletin (24) by Mr. Moorman provides an objective understanding of past work in this field, an experimental verification of the theory, and (best of all) a clarification of what the engineer may expect and should demand from the mathematician.

The paper fails to elaborate on the relation of stress to deflection; yet, because of the combination of longitudinal and rotational deformations, this subject is important, particularly in reinforced concrete design. The practicing engineer would stand defeated at this point even if the author's graphs would otherwise suit his needs. The paper would have been much more important if the author had attempted such an interesting problem.

In Appendix II, one of the books (19) seems to have no reference to the subject; two of them (3) (20) refer to mechanical engineering problems; and a fourth (1) is so broad and fundamental that it is the basis for all elastic problems. The writer does not consider these works proper for inclusion in the Bibliography on Curved Beams.

ENRICO VOLTERRA,[4] M. ASCE.—The writer thanks Mr. Oesterblom for contributing to the discussion of the paper.

---

[3] Rutherfordton, N. C.
[4] Prof. of Mechanics, Rensselaer Polytechnic Inst., Troy, N. Y.

The purpose of the paper was the study of deflections of circular beams in three particular and distinct cases: (1) Circular rings rigidly supported at symmetrical points and subjected to uniformly distributed forces; (2) circular-arc bow girders built in at both ends and subjected to uniformly distributed forces; and (3) circular-arc bow girders built in at both ends and subjected to concentrated forces.

Fig. 1 refers to case 1 of the circular ring and not to case 2 of the circular-arc bow girder (Fig. 2(*a*)) as erroneously interpreted by the discusser.

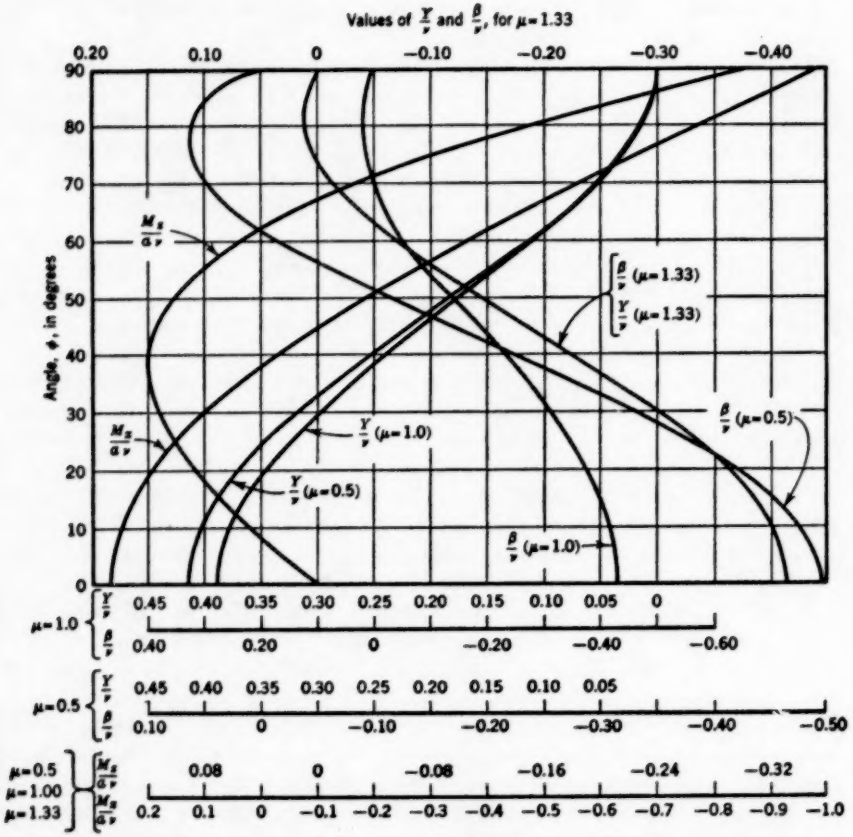

FIG. 12.—FUNCTIONS FOR A CIRCULAR-ARC BOW GIRDER WITH A DISTRIBUTED LOAD ($2\gamma = 180°$; AND $\mu = 0.5$, 1.0, AND 1.33)

Originally, the writer prepared many more graphs than those that were finally published; among the unpublished graphs were those for the case of circular-arc bow girders with a center angle $2\gamma = 180°$ to which Mr. Oesterblom refers. Graphs for this case are presented in Figs. 12 and 13.

The writer is aware of the works previously published on the subject, particularly those of English authors. He presented a bibliography which he thought was almost complete, containing all the works published on curved

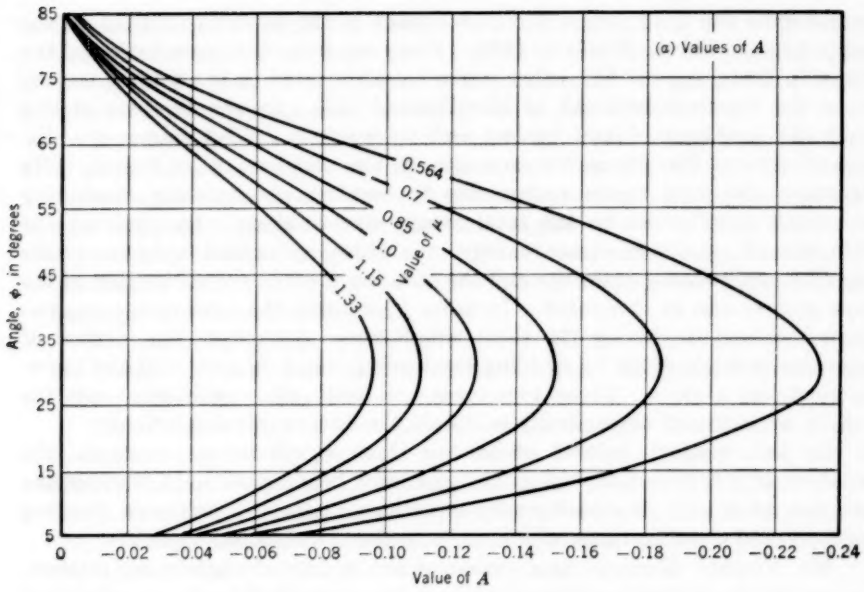

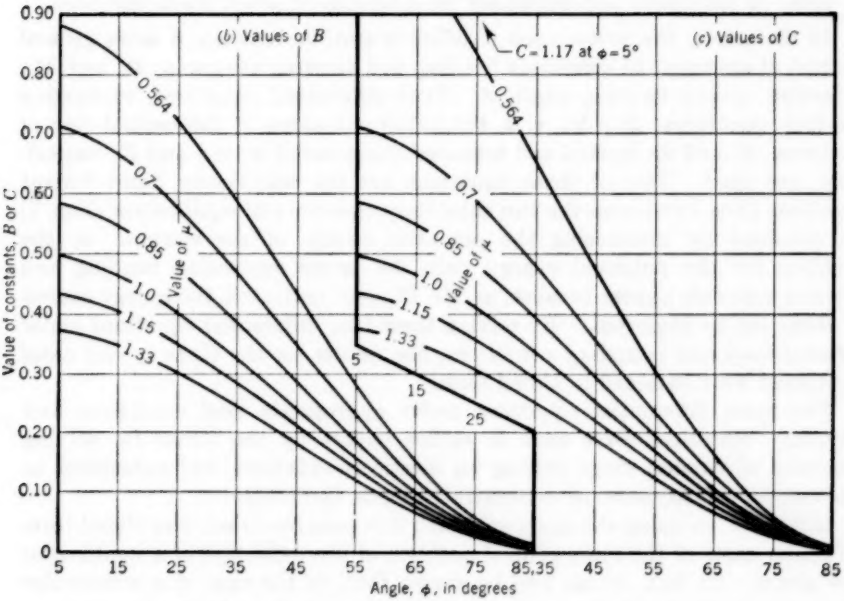

FIG. 13.—RELATIONSHIPS FOR A CIRCULAR-ARC BOW GIRDER WITH A CONCENTRATED LOAD ($2\gamma = 180°$)

beams from the 1843 papers of Saint-Venant to the papers published on the subject in the United States in 1950. However, since the presentation of the paper in the spring of 1952, other works have appeared on the subject, among them the excellent textbook of Mr. Pippard (25). In chapter nine of this book the problems of bow girders and transversely loaded frames are discussed (25*a*). Mr. Pippard's approach to the problems is as follows. He expresses the total strain energy due to bending and twisting, neglecting the small contribution to the total energy due to shear. By applying the principle of minimum strain energy, the three redundant unknowns—the bending and twisting moments and the shearing force in the midsection of the bow girder—can be computed. In order to simplify the numerical computations involved in solving the three simultaneous equations, the method of superposition is applied by dividing the loading into a symmetrical and skew-symmetrical system. These two cases are dealt with separately, and the results are summed algebraically to obtain the final required solutions.

By this method, instead of solving three simultaneous equations, the solution of a first equation gives the unknown bending moment whereas the solution of a pair of simultaneous equations yields the unknown twisting moment and shearing force, which can therefore be obtained explicitly.

Mr. Pippard discusses many cases of arc girders of engineering interest, among which are the cases of a circular-arc bow girder with a concentrated load and a circular-arc bow girder with a distributed load.

However, in the more general cases of noncircular-arc bow girders, Mr. Pippard finds that the resulting expressions

> "* * * cannot usually be integrated by exact mathematical process but must be calculated approximately by graphical or arithmetical methods."

In the paper, the writer used a different and, he believes, a more general method of approach to determine bending and twisting moments, M_x and M_z, deflection, v, and twisting angle, β. Four differential equations, connecting the four quantities, M_x, M_z, v, β, the initial curvature of the central line of the beam, R, and its inertial and torsional characteristics, $E\,I$ and K, respectively, are used. Two of these equations are the well-known Saint-Venant equations (Eqs. 1) whereas the two subsidiary equations of equilibrium (Eqs. 7) are obtained by minimizing the potential energy of the system. In the equation for the potential energy only the terms expressing bending and twisting moments appear because, as Mr. Pippard indicated, the energy caused by shear can be neglected. By solving these four differential equations under different load and boundary conditions, the results for the three special cases mentioned were obtained in closed form.

The same differential equations under appropriate load conditions and boundary conditions were used in earlier papers by the writer for solving problems of circular rings resting on elastic foundations and submitted to symmetric or antisymmetric concentrated loads (2)(21)(26).

Moreover, by using the same approach it is possible to solve in closed form particular cases of the more general problem of the deflection of a noncircular bow girder. In fact, it can also be shown that, in the case of a noncircular bow girder built-in at both ends and subjected to a uniformly distributed load,

the results can be expressed in closed form if the central line of the curved beam is a cycloid, a catenary, or a parabola. The writer is preparing a paper (1954) on the subject of deflections of noncircular bow girders in which the results for these special cases will be given in closed form.

Mr. Oesterblom's criticism that the paper fails to elaborate on the relation of stress to deflection is certainly not correct. In fact—as the formulas presented in the paper give in closed form the relationships existing among bending and twisting moments, deflections and angles of twist, initial curvatures, inertial and torsional characteristics of the beam, and external loading—it is possible in each specific case to derive from these formulas the relationships between stresses and deflections.

The textbook (19) to which the discusser refers as having no reference to the subject contains an entire chapter (Chapter XXI) dealing with small deformation of naturally curved rods (19*a*).

The two references (3) and (20), which according to the discusser apply to mechanical engineering problems and should not have been quoted, are Mr. Resal's fundamental work on bending and twisting of a curved beam and the textbook of S. Timoshenko, many pages (of the second volume) of which deal with the problem of bending of a curved beam out of its plane of initial curvature and give useful references on the entire subject.

Finally, the fourth work, which Mr. Oesterblom does not consider proper for inclusion in the bibliography on curved beams, is Saint-Venant's original papers (1). In these papers the theory of small deformations of initially curved beams was first developed.

Discussion of
"AN EXPERIMENTAL STUDY OF BUBBLES MOVING IN LIQUIDS"

By W. L. Haberman and R. K. Morton
(Proc. Sep. 387)

J. A. ROBERSON,[1] C. L. BARKER,[2] A.M. ASCE, and P. F. RUFF,[3] J.M. ASCE.—Messers. Haberman and Morton are to be complimented for their work concerning the movement of bubbles through liquids. Certainly their paper will be a definite contribution to the literature on this subject.

At the State College of Washington a study has been made by the writers of the movement of bubbles in a turbulent stream. It is interesting to note that close agreement exists between the results reported by the authors and those observed by the writers.

The problem of determining the rise velocity of bubbles, although somewhat academic to many becomes of great importance, e.g. in pipe lines where air is mechanically entrained. In lines of this type small bubbles tend to coalesce; and eventually form large air masses or "pockets." The removal of these air masses by pipe vents produces pressures that can be destructive. The problem of locating vents in a line for the removal of bubbles before they can form air masses, involved a study of bubble rise in a turbulent stream.

If U is the rise velocity, V the velocity of the water, and D the pipe diameter, the travel, L, of a bubble in rising a distance D is:

$$L = \frac{D}{V} U$$

In the study of vent location in pipe lines, L, in the above formula, is the distance the vent should be placed downstream from the point of entrance of the air bubbles into the pipe line, and U is the minimum rise velocity of the bubbles.

In the studies conducted by the writers, bubbles 1/4 inch in diameter or greater were studied. Davies[4] found the minimum rise velocity of bubbles of this size range, in a stationary liquid to be 0.6 feet per second. However, the problem with which the writers were concerned involved a liquid in a state of turbulence. An experimental apparatus was constructed of 5 1/2 inch lucite tubing to study the rise velocity of bubbles in a turbulent stream. The rise velocity, U, in a turbulent stream (Reynolds Number = 50,000 to 300,000) as determined by the writers agrees closely with the results obtained by Davies

1. Asst. Hydr. Engr., Div. of Industrial Research, and Instructor, Dept. of Civ. Eng., The State College of Washington, Pullman, Wash.
2. Prof. of Hydr. Eng., The State College of Washington, Pullman, Wash.
3. Junior Hydr. Engr., Div. of Industrial Research, and Instructor, Dept. of Civ. Eng., The State College of Washington, Pullman, Wash.
4. "The Mechanics of Large Bubbles Rising Through Extended Liquids and Through Liquids in Tubes", by R. M. Davies and G. I. Taylor, Proceedings, Royal Society of London, Vol. 200, Series A, 1950.

and the authors. Precise comparison was not practical because of the variations above and below the mean rise velocity as a result of turbulence.

It was of interest to the writers to note that the data of Figure 2, of the authors' paper, plotted a smooth curve. The results presented by Davies, as did the writers, gave a spread of points, especially for the bubbles of relatively large diameter.

CORRECTION TO DISCUSSION OF APPLICATIONS OF THE RELAXATION TECHNIQUE IN FLUID MECHANICS

(Proc. Sep. 223)

The name of Mladen Boreli was misspelled on the inside front cover and on page 396-3.

CORRECTION TO DISCUSSION OF MECHANICS OF MANIFOLD FLOW

(Proc. Sep. 258)

On page 396-22, in the first term of the right-hand member of Eq. 4, the squared quantity should be summed to $\underline{i}$ for each value of i before summing the entire system to n-1.

PROCEEDINGS-SEPARATES

The technical papers published in the past year are presented below. Technical-division sponsorship is indicated by an abbreviation at the end of each Separate Number, the symbols referring to: Air Transport (AT), City Planning (CP), Construction (CO), Engineering Mechanics (EM), Highway (HW), Hydraulics (HY), Irrigation and Drainage (IR), Power (PO), Sanitary Engineering (SA), Soil Mechanics and Foundations (SM), Structural (ST), Surveying and Mapping (SU), and Waterways (WW) divisions. For titles and order coupons, refer to the appropriate issue of "Civil Engineering" or write for a cumulative price list.

VOLUME 80 (1954)

JANUARY: 379(SM)[c], 380(HY), 381(HY), 382(HY), 383(HY), 384(HY)[c], 385(SM), 386(SM), 387(EM), 388(SA), 389(SU)[c], 390(HY), 391(IR)[c], 392(SA), 393(SU), 394(AT), 395(SA)[c], 396(EM)[c], 397(ST)[c].

FEBRUARY: 398(IR)[d], 399(SA)[d], 400(CO)[d], 401(SM)[c], 402(AT)[d], 403(AT)[d], 404(IR)[d], 405(PO)[d], 406(AT)[d], 407(SU)[d], 408(SU)[d], 409(WW)[d], 410(AT)[d], 411(SA)[d], 412(PO)[d], 413(HY)[d].

MARCH: 414(WW)[d], 415(SU)[d], 416(SM)[d], 417(SM)[d], 418(AT)[d], 419(SA)[d], 420(SA)[d], 421(AT)[d], 422(SA)[d], 423(CP)[d], 424(AT)[d], 425(SM)[d], 426(IR)[d], 427(WW)[d].

APRIL: 428(HY)[c], 429(EM)[c], 430(ST), 431(HY), 432(HY), 433(HY), 434(ST).

MAY: 435(SM), 436(CP)[c], 437(HY)[c], 438(HY), 439(HY), 440(ST), 441(ST), 442(SA), 443(SA).

JUNE: 444(SM)[e], 445(SM)[e], 446(ST)[e], 447(ST)[e], 448(ST)[e], 449(ST)[e], 450(ST)[e], 451(ST)[e], 452(SA)[e], 453(SA)[e], 454(SA)[e], 455(SA)[e], 456(SM)[e].

JULY: 457(AT), 458(AT), 459(AT)[c], 460(IR), 461(IR), 462(IR), 463(IR)[c], 464(PO), 465(PO)[c].

AUGUST: 466(HY), 467(HY), 468(ST), 469(ST), 470(ST), 471(SA), 472(SA), 473(SA), 474(SA), 475(SM), 476(SM), 477(SM), 478(SM)[c], 479(HY)[c], 480(ST)[c], 481(SA)[c], 482(HY), 483(HY).

SEPTEMBER: 484(ST), 485(ST), 486(ST), 487(CP)[c], 488(ST)[c], 489(HY), 490(HY), 491(HY)[c], 492(SA), 493(SA), 494(SA), 495(SA), 496(SA), 497(SA), 498(SA), 499(HW), 500(HW), 501(HW)[c], 502(WW), 503(WW), 504(WW)[c], 505(CO), 506(CO)[c], 507(CP), 508(CP), 509(CP), 510(CP), 511(CP).

OCTOBER: 512(SM), 513(SM), 514(SM), 515(SM), 516(SM), 517(PO), 518(SM)[c], 519(IR), 520(IR), 521(IR), 522(IR)[c], 523(AT)[c], 524(SU), 525(SU)[c], 526(EM), 527(EM), 528(EM), 529(EM), 530(EM)[c], 531(EM), 532(EM)[c], 533(PO).

NOVEMBER: 534(HY), 535(HY), 536(HY), 537(HY), 538(HY)[c], 539(ST), 540(ST), 541(ST), 542(ST), 543(ST), 544(ST), 545(SA), 546(SA), 547(SA), 548(SM), 549(SM), 550(SM), 551(SM), 552(SA), 553(SM)[c], 554(SA), 555(SA), 556(SA), 557(SA).

DECEMBER: 558(ST), 559(ST), 560(ST), 561(ST), 562(ST), 563(ST)[c], 564(HY), 565(HY), 566(HY), 567(HY), 568(HY)[c], 569(SM), 570(SM), 571(SM), 572(SM)[c], 573(SM)[c], 574(SU), 575(SU), 576(SU), 577(SU), 578(HY), 579(ST), 580(SU), 581(SU), 582(Index).

VOLUME 81 (1955)

JANUARY: 583(ST), 584(ST), 585(ST), 586(ST), 587(ST), 588(ST), 589(ST)[c], 590(SA), 591(SA), 592(SA), 593(SA), 594(SA), 595(SA)[c], 596(HW), 597(HW), 598(HW)[c], 599(CP), 600(CP), 601(CP), 602(CP), 603(CP), 604(EM), 605(EM), 606(EM)[c], 607(EM).

---

c. Discussion of several papers, grouped by Divisions.
d. Presented at the Atlanta (Ga.) Convention of the Society in February, 1954.
e. Presented at the Atlantic City (N.J.) Convention in June, 1954.

AMERICAN SOCIETY OF CIVIL ENGINEERS

OFFICERS FOR 1955

PRESIDENT

WILLIAM ROY GLIDDEN

VICE-PRESIDENTS

Term expires October, 1955:
ENOCH R. NEEDLES
MASON G. LOCKWOOD

Term expires October, 1956:
FRANK L. WEAVER
LOUIS R. HOWSON

DIRECTORS

Term expires October, 1955:
CHARLES B. MOLINEAUX
MERCEL J. SHELTON
A. A. K. BOOTH
CARL G. PAULSEN
LLOYD D. KNAPP
GLENN W. HOLCOMB
FRANCIS M. DAWSON

Term expires October, 1956:
WILLIAM S. LaLONDE, JR.
OLIVER W. HARTWELL
THOMAS C. SHEDD
SAMUEL B. MORRIS
ERNEST W. CARLTON
RAYMOND F. DAWSON

Term expires October, 1957:
JEWELL M. GARRELTS
FREDERICK H. PAULSON
GEORGE S. RICHARDSON
DON M. CORBETT
GRAHAM P. WILLOUGHBY
LAWRENCE A. ELSENER

PAST-PRESIDENTS

Members of the Board

WALTER L. HUBER
DANIEL V. TERRELL

EXECUTIVE SECRETARY

WILLIAM N. CAREY

ASSISTANT SECRETARY

E. L. CHANDLER

TREASURER

CHARLES E. TROUT

ASSOCIATE SECRETARY

WILLIAM H. WISELY

ASSISTANT TREASURER

CARLTON S. PROCTOR

PROCEEDINGS OF THE SOCIETY

HAROLD T. LARSEN
Manager of Technical Publications

DEFOREST A. MATTESON, JR.
Editor of Technical Publications

PAUL A. PARISI
Assoc. Editor of Technical Publications

COMMITTEE ON PUBLICATIONS

SAMUEL B. MORRIS, *Chairman*

JEWELL M. GARRELTS, *Vice-Chairman*

GLENN W. HOLCOMB
OLIVER W. HARTWELL
ERNEST W. CARLTON
DON M. CORBETT